



C3 amino-substituted chalcone derivative with selective adenosine rA_1 receptor affinity in the micromolar range

Helena D. Janse van Rensburg¹ · Lesetja J. Legoabe¹ · Gisella Terre'Blanche^{1,2}

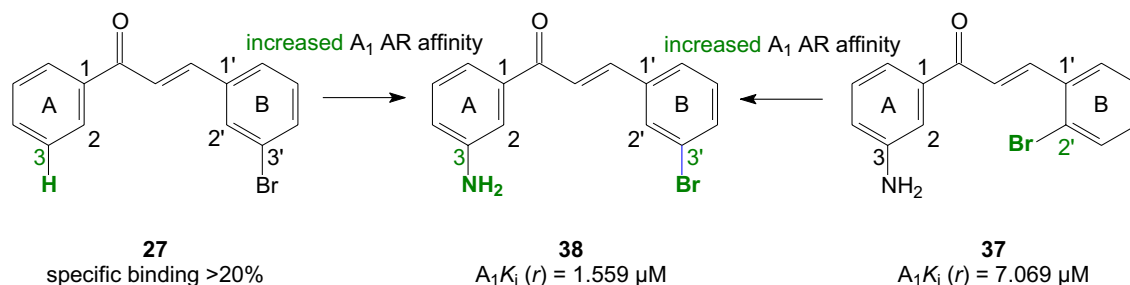
Received: 10 March 2020 / Accepted: 3 November 2020 / Published online: 17 November 2020
© Institute of Chemistry, Slovak Academy of Sciences 2020

Abstract

To identify novel adenosine receptor (AR) ligands based on the chalcone scaffold, herein the synthesis, characterization and in vitro and in silico evaluation of 33 chalcones (**15–36** and **37–41**) and structurally related compounds (**42–47**) are reported. These compounds were characterized by radioligand binding and GTP shift assays to determine the degree and type of binding affinity, respectively, against rat (*r*) A_1 and A_{2A} ARs. The chalcone derivatives **24**, **29**, **37** and **38** possessed selective A_1 affinity below 10 μM , and thus, are the most active compounds of the present series; compound **38** was the most potent selective A_1 AR antagonist ($K_i(r) = 1.6 \mu\text{M}$). The structure–affinity relationships (SAR) revealed that the NH_2 -group at position C3 of ring A of the chalcone scaffold played a key role in affinity, and also, the Br-atom at position C3' on benzylidene ring B. Upon in vitro and in silico evaluation, the novel C3 amino-substituted chalcone derivative **38**—that contains an α,β -unsaturated carbonyl system and easily allows structural modification—may possibly be a synthon in future drug discovery.

Graphic abstract

C3 amino-substituted chalcone derivative (**38**) with C3' Br substitution on benzylidene ring B possesses selective adenosine rA_1 receptor affinity in micromolar range.



Keywords Chalcone · Schiff base · Base- and acid-catalysed Claisen–Schmidt condensation reactions · Selective adenosine A_1 receptor antagonist · Neurological conditions

Electronic supplementary material The online version of this article (<https://doi.org/10.1007/s11696-020-01414-9>) contains supplementary material, which is available to authorized users.

✉ Lesetja J. Legoabe
Lesetja.Legoabe@nwu.ac.za

¹ Centre of Excellence for Pharmaceutical Sciences, North-West University, Private Bag X6001, Potchefstroom 2520, South Africa

² Pharmaceutical Chemistry, School of Pharmacy, North-West University, Private Bag X6001, Potchefstroom 2520, South Africa

Introduction

In the human body, adenosine takes part in both physiologic and pathophysiologic processes (Boison 2018). Most, if not all, of these actions are mediated by four cell surface receptors, denoted A_1 , A_{2A} , A_{2B} and A_3 (Fredholm et al. 1994, 2001, 2011). Ensuing almost 100 years of research on adenosine and its receptors as well as the ligands that bind to these adenosine receptors (ARs), the potential of the adenosine

system as a drug discovery target is evident (de Lera Ruiz et al. 2013).

The A₁ AR has been cloned from different mammalian species, including humans (Müller 2001) and show structural homology among diverse mammalian species (Ralevic and Burnstock 1998) (although lower affinity for human than rat receptors have been reported) (Klotz et al. 1997). A member of the seven transmembrane-spanning G-protein-coupled receptor superfamily (that preferentially couples to inhibitory G_{i/o} heterotrimeric G-proteins) (Freissmuth et al. 1991; Munshi et al. 1991; Ralevic and Burnstock 1998), the A₁ AR inhibits adenylate cyclase and decreases cyclic adenosine monophosphate (Londos et al. 1980; Van Calker et al. 1978). Other second messenger systems may also be coupled to the A₁ AR, such as phospholipase C and several types of calcium and potassium channels (Ralevic and Burnstock 1998). A₁ ARs are widely distributed in different mammalian species (Ralevic and Burnstock 1998) and ubiquitous within the central nervous system, with the highest density in the cerebral cortex, cerebellum, hippocampus, thalamus, brainstem and spinal cord (Dixon et al. 1996; Reppert et al. 1991). These receptors are localized in the active zone of the presynaptic nerve terminal (Rebola et al. 2003; Swanson et al. 1995), a highly specialized region of the cytoplasm that directly faces the synaptic cleft (Sankaranarayanan and Ryan 2007).

At presynaptic nerve terminals, A₁ ARs play a role in the release of neurotransmitters (Dunwiddie 1985). Adenosine acts by inhibiting cholinergic transmission, among other, via A₁ ARs (Phillis 1991). The cholinergic system has been associated with a number of cognitive functions, for example, learning and memory as well as emotion (Jackson 2011).

Interaction between the adenosine and cholinergic system is regrettably controversial; on the one hand, administration of a selective A₁ AR agonist (e.g. CPA) caused learning and memory deficits, which may be prevented by a selective A₁ AR antagonist (e.g. DPCPX) (Normile and Barraco 1991), and on the other hand, the said antagonist also caused learning and memory deficits (Vollert et al. 2013)! Moreover, it was found that chronic treatment with A₁ AR modulators result in behavioural effects different from those observed following acute administration; therefore, particular caution is required in the development of adenosine-based strategies for the chronic treatment of neurodegenerative or cognitive disorders (Von Lubitz et al. 1993). Other studies advocated the use of A₁ AR antagonists and considered the A₁ AR an interesting drug target for the development of cognitive enhancers based on the observation that A₁ AR antagonism positively modulated memory process (Maemoto et al. 2004; Normile and Barraco 1991; Pitsikas and Borsini 1997; Suzuki et al. 1993).

Apart from learning and memory, adenosine and its receptors—specifically the A₁ AR—also modulate anxiety where blockade of the A₁ AR results in anxiolytic actions (Maemoto et al. 2004). The A₁ AR agonist R-PIA exacerbated the effects of ethanol withdrawal, whereas the A₁ AR antagonist CPT improved these anxiogenic effects in the elevated plus-maze and light/dark test, relevant behavioural animal models of anxiety (Gatch et al. 1999). These results suggest that A₁ AR antagonists, at some doses, may be useful for ameliorating the anxiogenic effects produced by ethanol withdrawal, although it does not appear useful for reducing ethanol consumption (Gatch et al. 1999). Furthermore, the widely used anxiolytic agents, benzodiazepines, block adenosine uptake (Noji et al. 2004) and decreased A₁ AR binding capacity in vivo at doses of clinical relevance (Kaplan et al. 1992). As with the adenosine system and its effects on learning and memory, there is controversy: DPCPX did not affect the anxiety state of mice in the elevated plus-maze test (Jain et al. 1995) and A₁ AR knockout mice showed signs of increased anxiety in the light/dark test (Johansson et al. 2001).

Adenosine and its analogues have been known to cause behavioural despair in animal models relevant to depression. The A_{2A}, rather than the A₁, AR is involved in depression; based on evidence from pharmacology and A_{2A} AR knockout mice (Yacoubi et al. 2001). (Additionally, the selective A_{2A} AR antagonist istradefylline not only improves motor fluctuations but also some non-motor symptoms of Parkinson's disease (PD); such as the mood disorder depression—the most common non-motor symptom of PD (Aarsland et al. 2012; Nagayama et al. 2019) This is yet to be confirmed by a double-blind placebo-controlled trial (Nagayama et al. 2019). Interestingly, the selective A₁ AR antagonist DPCPX enhanced the anti-depressant effects of selective serotonin re-uptake inhibitors (SSRIs) imipramine, escitalopram and reboxetine in mice behavioural tests (Szopa et al. 2018); nevertheless, the effects of atypical antidepressants agomelatine and tianeptine were increased, not by DPCPX, but by the selective A_{2A} AR antagonist DMPX (Szopa et al. 2019).

The orally active and brain penetrable pyrazolopyridine derivative FR194921 (**1**) exhibits potent affinity for the A₁ AR (A₁ (*h*) K_i = 2.9 nM) without affinity for the A_{2A} and A₃ ARs (Fig. 1). In addition, no species differences among human, rat and mouse were observed in the binding affinity profile of this compound (Maemoto et al. 2004). After oral administration of FR194921 (**1**), hypolocomotion in rats caused by the A₁ AR agonist CPA was bettered demonstrating A₁ AR antagonism in vivo (Maemoto et al. 2004). Additionally, scopolamine-induced memory deficits (passive avoidance test) as well as anxiety (social interaction test and elevated plus-maze test) were also bettered by the said compound (**1**), without influencing general behaviour (Maemoto

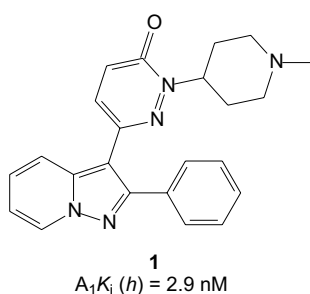


Fig. 1 The chemical structure and $A_1K_i(h)$ value (nM) of FR194921 (**1**)

et al. 2004). FR194921 (**1**) showed no anti-depressant activity (forced swim test)—even at high doses. It may be said that FR194921 (**1**) shows promise in the treatment of memory deficits and anxiety (Maemoto et al. 2004).

The role of A_1 AR antagonists in brain functioning is not yet fully understood, and at times, debatable—yet, selective A_1 AR antagonists have potential for the treatment of neurological and psychiatric conditions, as seen with the potent and selective A_1 AR antagonist FR184921 (**1**).

While diverse classes of A_1 AR antagonists have been documented since the discovery of the receptor and specific radiolabelled ligands, most of these compounds were derived from xanthine analogues which show poor water solubility and oral bioavailability, central nervous system penetration and considerable species differences in terms of receptor binding affinity (Maemoto et al. 1997). Due to these undesirable physicochemical properties of xanthine derivatives, the focus has shifted from xanthine to non-xanthine based heterocycles as A_1 AR antagonists (de Lera Ruiz et al. 2013).

The chemical structure 1,3-diphenyl-2-propen-1-one—perhaps better known by the general term “chalcone”—has attracted attention from both chemical (biosynthesis and synthesis) and biological standpoints; due to the wide-ranging pharmacological properties exhibited by these compounds (Mathew et al. 2019; Zhuang et al. 2017). These properties include anticancer, antileishmanial, anti-malarial, antimicrobial, antiviral, antifungal, antioxidant, antihypertensive and antidiabetic biological activities—to name a few (Batovska and Todorova 2010; Sahu et al. 2012; Karthikeyan et al. 2015; Singh et al. 2014; Zhou and Xing 2015). Additionally, chalcones show potential in the treatment of neurological conditions by acting as anxiolytics and antidepressants, as well as the modulation of gamma-aminobutyric acid (GABA) receptors and the inhibition of acetylcholinesterase (AChE), butyrylcholinesterase (BChE) and monoamine oxidase (MAO) (Mathew et al. 2019). Of note, the chalcone–coumarin hybrid (**2**) possesses selective A_3 AR affinity ($A_3K_i(h) = 5.2 \mu\text{M}$)

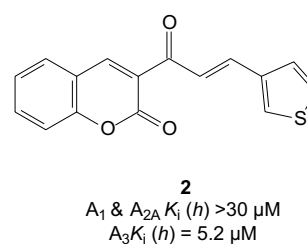


Fig. 2 The chemical structure and A_1 , A_{2A} and $A_3K_i(h)$ values of **2**

(Vazquez-Rodriguez et al. 2013), the blockade of A_3 ARs may be advantageous in brain ischemia (Fig. 2) (Jacobson and Gao 2006).

The term chalcone generally refers to chemicals with an α,β -unsaturated carbonyl system; thus, the chalcone family has extensive structural diversity (Zhuang et al. 2017). For example, the chalcone-based benzocycloalkanone derivatives are hybrid chalcones with the core scaffold of 1,3-diaryl-2-propen-1-one (Fig. 3). Some of these compounds structurally related to chalcones include aurone derivatives, which also possess selective A_1 affinity [such as hispidol (**3**)] (Jacobson et al. 2002) and served as inspiration for the structurally related 2-benzylidene-1-tetralone (**4–8**) (Janse van Rensburg et al. 2017; Legobe et al. 2018) and 2-benzylidene-1-indanone derivatives (**9–12**) (Janse van Rensburg et al. 2019a, b), leading to compounds with selective affinity for the A_1 AR in the micromolar range.

The chemistry of chalcones is as attractive today as it was years ago; due to the open-chain model and the feature of skeletal modification to produce a new class of organic compounds such as isoxazole-, pyrazole- and indole-based chalcones. Heterocycles occupy a central position in medicinal chemistry and a number of both approved and potential drugs contain at least one heterocyclic nucleus (Khanam 2015; McGrath et al. 2010). Based on the above and in continuation of the efforts to obtain heterocycles as A_1 and/or A_{2A} AR antagonists, simple chalcone derivatives (**15–36**) with either ring A or ring B substitutions as well as a series of novel C3 amino-substituted chalcone derivatives (**37–41**) with halogen (Br-, Cl- and F-atoms) substitutions on ring B and their regioisomers (**42–47**) were designed containing the basic chalcone scaffold as structural core. Herein the synthesis, characterization and evaluation, both in vitro and in silico, will be discussed to ascertain the structure–affinity relationships (SAR) that govern A_1 and/or A_{2A} AR affinity as well as the future of the said compounds as synthons by which a range of analogues may be designed for future drug discovery.

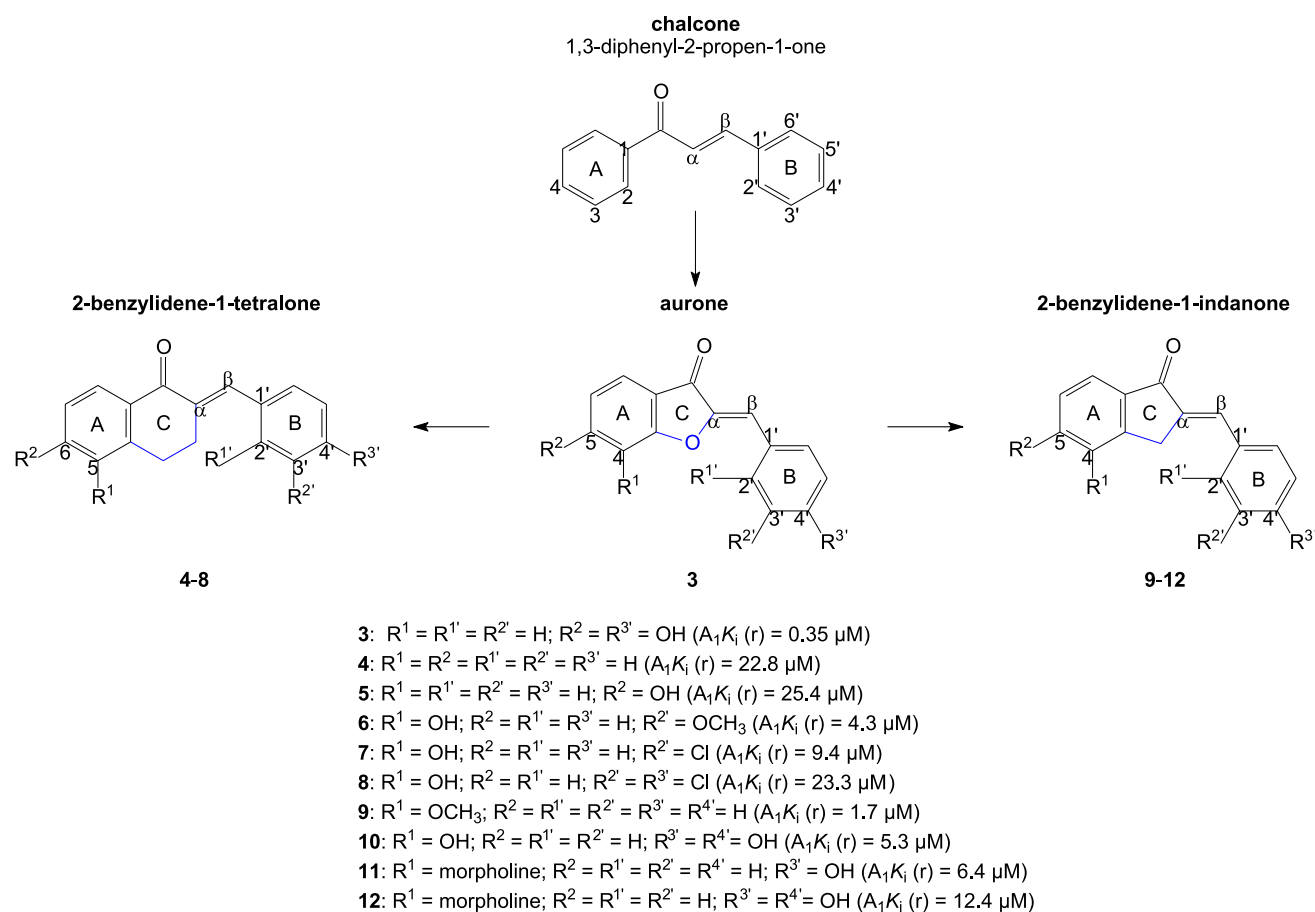


Fig. 3 The chemical structure and A_1K_i (r) values of aurone (**3**), 2-benzylidene-1-tetralone (**4–8**) and 2-benzylidene-1-indanone (**9–12**) derivatives

Results and discussion

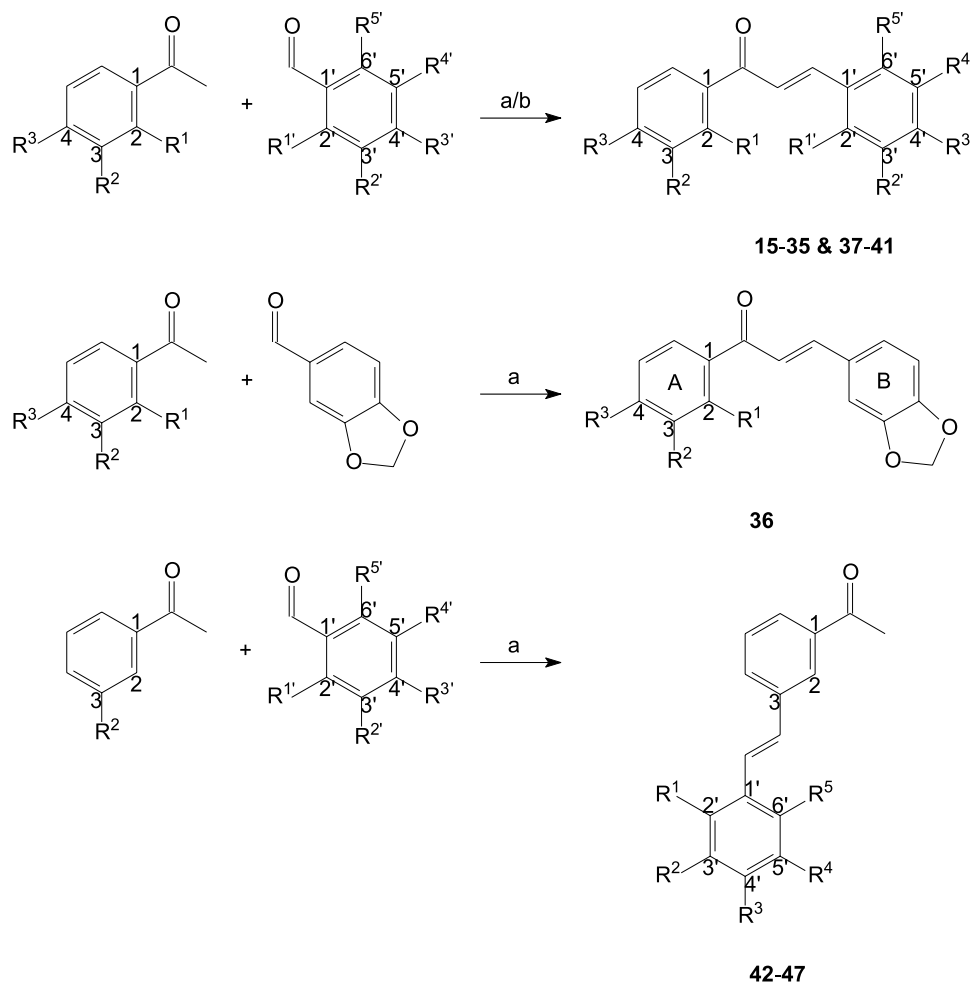
Chemistry

The synthesis of the chalcone derivatives **15–36** and **37–41** was done by a Claisen–Schmidt condensation reaction (Claisen and Claparède 1881; Schmidt 1881) of acetophenone and benzaldehyde using either a base or an acid catalyst in a polar solvent (Fig. 4a, b)—this well-known synthetic route is deemed a classical organic chemistry reaction. As stated, the condensing agents are either strong bases or acids (generally, basic conditions are more common in chalcone synthesis) (Gaonkar and Vignesh 2017; Gomes et al. 2017; Rammohan et al. 2020; Zhuang et al. 2017); in the case of base catalysts (**15–36**), the chalcone is generated from the aldol product via dehydration in an enolate mechanism, while in the case of acid catalysts (**37–41**), the chalcone is generated via an enol mechanism (Nielsen and Houlihan 2004; Noyce and Pryor 1955). The Claisen–Schmidt condensation reaction is widespread in the literature because of its experimental simplicity and

highly efficient formation of the carbon–carbon double bond.

The synthesis of the Schiff base or imine derivatives **42–47** by condensation of 3-aminoacetophenone and different substituted benzaldehydes using a base catalyst in a polar solvent (Fig. 4a)—analogous to the reaction conditions of chalcone derivatives **15–36**—was not planned. Initially, it was thought that the said reaction conditions would yield compounds **37–41** and not the regioisomers of these C3 amino-substituted chalcone derivatives comprised of two aromatic rings linked via an azomethine (C=N) group. Schiff base or imine compounds are formed by the reaction of a primary amine (such as 3-aminoacetophenone) and either aldehydes (such as the different substituted benzaldehydes) or ketones with the simultaneous removal of water (Furniss et al. 1989). When one, or both, of the reactants are aromatic, the imine is quite stable and usually known as a Schiff base, additionally, in the case of wholly aliphatic reactants the imines tend to decompose or polymerise (Furniss et al. 1989).

Fig. 4 Synthesis of **15–36**, **37–41** and **42–47** (R substituents are identified in Tables 2, 3, 4). Reagents and conditions: **a** EtOH, KOH (10% (w/v) aqueous solution), room temperature; **b** MeOH, HCl (32 wt. % in H₂O, FCC), 120 °C



Under the adopted synthetic routes, the test compounds **15–36**, **37–41** and **42–47** were obtained in fair to good yields, purified by recrystallization from a suitable solvent (EtOH), and in the instance of compounds **37–41** and **42–47**, the structure, molecular mass and/or purity of these compounds were verified by ¹H NMR, ¹³C NMR, MS and/or HPLC (Supplementary data). The known chalcone derivatives **15–36** were characterized by ¹H NMR only, melting point (DSC) and HPLC and are in accordance with the literature values.

Taking the novel 3-amino-substituted chalcone derivative **38** (R² = NH₂; R^{2'} = Br) as a representative case, the ¹H NMR spectrum displayed two characteristic signals for the ethylenic protons H_α (nearer the carbonyl group) and H_β (next to the H_α proton) at 7.73 and 7.97 ppm, respectively, as doublets (*J*_{H_α,H_β} = 15.7 Hz). Protons on the NH₂-group (similar to the proton on the OH-group) are not always visible on a ¹H NMR spectrum as protons attached to a N-atom (or O-atom) are acidic, and thus, exchangeable. Also, the ¹³C NMR spectrum displayed three characteristic signals: a prominent signal for the carbonyl group at 188.36 ppm

and two other signals typical of C_α (121.39 ppm) and C_β (142.81 ppm).

From the coupling constant value of the ethylenic protons H_α and H_β (*J*_{H_α,H_β} = 15.7 Hz), it may be deduced that compound **38** exists in the *trans* (*E*) configuration (Aksöz and Ertan 2012; Barros et al. 2004; Jung et al. 2008; Opletalova et al. 2000; Rao et al. 2001, 2004). As a result of the diamagnetic anisotropy (deshielding of proton due to local diamagnetic current) of the carbonyl functional group, the ethylenic proton of the (*E*) isomer gave a signal at a greater chemical shift than the ethylenic proton of the (*Z*) isomer, as the latter is more remote from the carbonyl functional group (Bayer et al. 1991). Stereochemically, a chalcone might exist as either a *cis* (*Z*)- or *trans* (*E*)-isomer, having two aromatic rings linked via a three carbon α,β-unsaturated carbonyl system (Gomes et al. 2017; Hallgas et al. 2005). The *cis* (*Z*)-conformer is thermodynamically less stable than the *trans* (*E*)-conformer due to the steric effects between the carbonyl group and ring A (Hallgas et al. 2005; Van der Werden et al. 1995). The more stable *trans* (*E*)-isomer is the predominant configuration among chalcones (Gomes et al. 2017).

The mass spectrum of compound **38** displayed an intense $[M + H]^+$ molecular ion peak at 302.0164 (^{79}Br isotope) as well as an intense $[M + H]^{+2}$ peak at 304.0152 (^{81}Br isotope)—in accordance with the formulation depicted ($\text{C}_{15}\text{H}_{13}\text{BrNO}$). Since Bromine has two isotopes (in a ratio of approximately 1:1), a compound containing a Br-atom (such as compounds **37–38**) will have two peaks of similar height in the molecular ion region depending on which bromine isotope the molecular ion contains. Additionally, the two M^+ molecular ion peaks for compound **38** ($\text{C}_{15}\text{H}_{12}\text{BrNO}$) may be seen at 301.0096 (^{79}Br isotope) and 303.0095 (^{81}Br isotope). Of note, chlorine also has two isotopes, namely ^{35}Cl and ^{37}Cl (in a ratio of 3:1) meaning a similar effect may be observed on the mass spectrum of an organic compound containing a Cl-atom (for example, compounds **39–40**). The purity of compound **38** determined by HPLC was 98.0549%. The melting point of compound **38** determined by DSC was 176.78 °C.

The word chalcone is derived from the Greek word “chalcos”, meaning “bronze”, which results from the colours of most natural chalcones (Sahu et al. 2012). The bronze colour of chalcones is most likely due to the reactive keto-ethylenic group $\text{CO}-\text{CH}=\text{CH}-$; a chromophore responsible for the colour of chalcones depending on the presence of other auxochromes (Gaonkar and Vignesh 2017). This bronze colour scheme was also observed with most of the synthesised chalcones, for example, the light brown colour of **38**.

As stated, the 3-amino-substituted chalcones and the Schiff base derivatives **42–47** are regioisomers (*molecules* with the same *molecular formula*, but different bonding patterns and atomic organisations), and as such, dissimilarities were detected on the ^1H NMR and ^{13}C NMR spectra when comparing these compounds. The absence of the ethylenic protons H_α and H_β may be observed on the ^1H NMR spectrum and the signals typical of C_α and C_β , on the ^{13}C NMR. In the place of these signals, the proton adjacent to the azomethine group was visible on the ^1H NMR spectrum and the carbon of the azomethine group on the ^{13}C NMR spectrum. Additionally, on both the ^1H NMR and ^{13}C NMR spectra the methyl group from the acetophenone moiety was clearly visible downfield of all other signals.

Biology

In vitro evaluation

Radioligand binding assays

The degree of binding affinity that the test compounds showed toward rat (r) A_1 and A_{2A} ARs were determined via radioligand binding assays in either duplicate [specific binding (%)] or triplicate [inhibition constant (K_i , μM)]

and expressed as either mean or mean \pm standard error of the mean (SEM), respectively. Only compounds **24**, **29**, **37** and **38**—which displayed specific binding values $< 20\%$ at a maximum tested concentration of 100 μM —justified the determination of inhibition constant values (K_i , μM), unlike compounds **15–23**, **25–28**, **30–36**, **39–41** and **42–47** (specific binding values $> 20\%$). The radioligand binding assays were validated with CPA (A_1 agonist), DPCPX (A_1 antagonist) and istradefylline (A_{2A} antagonist) as reference compounds and results were in accordance with literature values (Table 1).

Structure–affinity relationships (SAR)

As depicted in Tables 2, 3 and 4, most of the test compounds showed poor A_1 and/or A_{2A} AR affinity upon in vitro evaluation—making it difficult to determine SAR; however, some broad conclusions may be drawn from these results. In brief, the test compounds were noticeably more active against the A_1 AR than A_{2A} AR and the chalcone derivatives **24**, **29**, **37** and **38** showed selective A_1 AR affinity below 10 μM —of these compounds, **38** had the best A_1 AR affinity (A_1K_i (r) = 1.6 μM). The type of substitution on ring A of the chalcone scaffold played a key role in affinity, and also, the type and position of the substitution on benzylidene ring B.

As stated, the chalcone derivatives **24** (A_1K_i (r) = 5.3 μM) and **29** (A_1K_i (r) = 6.1 μM) (Table 2) showed selective A_1 AR affinity below 10 μM , and although, the K_i (r) values of these compounds were quite similar the substitutions on ring B were not; **24** was C2', C4', C5'-trimethoxy substituted and **29** was C2'-chloro substituted. In the past, the antimicrobial (Karaman et al. 2010; Ramyashree et al. 2017), anticancer (Juvale et al. 2012; Mellado et al. 2018) and/or antioxidant (Shenvi et al. 2013) activities of compounds **24** and **29** were also explored, and now, selective A_1 AR affinity may be added.

With regard to compound **24** and A_1 AR affinity, it seems that the C2', C4', C5' substitution pattern on ring B was preferred to that of compound **25** ($[^3\text{H}]\text{DPCPX}$ -specific binding (r) = 27%)—interestingly, these compounds differ only at the C5' (**24**: $-\text{OCH}_3$; **25**: $-\text{H}$) and C6' (**24**: $-\text{H}$; **25**: $-\text{OCH}_3$) positions. However, the radioligand-specific binding against the A_{2A} AR of these compounds were the same (**24–25**: $[^3\text{H}]\text{NECA}$ -specific binding (r) = 28%). Comparison of **24** to the structurally related 2-benzylidene-1-indanone compound **13** (Fig. 5) consisting of a fused 6- and 5-membered ring system (ring A and ring C, respectively) along with C4'-methoxy substitution on ring A had poor A_1 and A_{2A} AR affinity (Janse van Rensburg et al. 2019b). The decreased affinity may be due to the increased number of C-, H- and O atoms in the form of the C4 OCH_3 -group substitution on ring A and the CH_2 -group present in ring C, increasing the molecular weight from 298.34 g/mol (**24**) to 340.38 g/

Table 1 K_i values for the binding affinity of reference compounds against rat (*r*) A_1 and A_{2A} ARs

#	$K_i \pm \text{SEM}$ (μM) ^a			SI ^g	GTP shift ^h
	<i>rA</i> ₁ ^b vs [³ H]DPCPX ^d	<i>rA</i> _{2A} ^c vs [³ H]NECA ^e	<i>rA</i> ₁ ^c + GTP ^f vs [³ H]DPCPX ^d		
CPA (A_1 agonist)	0.0057 ± 0.0015 (0.0068) ⁱ (0.015) ^j (0.0079) ^k	0.40 ± 0.17 (0.16) ⁱ (0.33) ^j	0.099 ± 0.015 (0.099) ⁱ (0.099) ^j	70 (24) (22)	17 (15) ⁱ (14) ^j
DPCPX (A_1 antagonist)	0.0005 ± 0.00003 (0.0004) ⁱ (0.0005) ^j (0.0003) ^l	0.23 ± 0.03 (0.55) ⁱ (0.53) ^j (0.34) ^l	0.0006 ± 0.00003 (0.0004) ⁱ (0.0004) ^j	468 (1362) (1060) (1133)	1.2 (1) ⁱ (1.3) ^j
Istradefylline (A_{2A} antagonist)	0.19 ± 0.01 (0.23) ^m	0.0014 ± 0.0003 (0.0022) ^m	0.15 ± 0.02	7.3 (0.0096)	0.79

^aAll inhibition constant (K_i) values were determined in triplicate and expressed as mean ± standard error of the mean (SEM) in μM

^bRat receptors were used (*rA*₁: rat whole brain membranes)

^cRat receptors were used (*rA*_{2A}: rat striatal membranes)

^d0.1 nM [³H]DPCPX

^e4 nM [³H]NECA

^fAddition of 100 μM GTP to A_1 AR radioligand binding assay

^gSelectivity index (SI) for the A_1 AR isoform calculated as a ratio of $A_{2A}K_i/A_1K_i$

^hGTP shift calculated by dividing K_i value in the presence of 100 μM GTP by K_i value in the absence of 100 μM GTP

ⁱLiterature value obtained from (Janse van Rensburg et al. 2017)

^jLiterature value obtained from (Van der Walt and Terre'Blanche 2015)

^kLiterature value obtained from (Bruns et al. 1987)

^lLiterature value obtained from (Lohse et al. 1987)

^mLiterature value obtained from (Shimada et al. 1997)

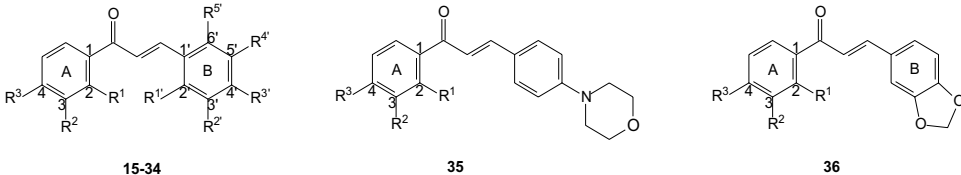
mol (**13**), and perhaps, the resultant steric hindrance (of the CH_2 -group present in ring C and $\text{C}2'$ OCH_3 -group on ring B) also decreased binding affinity (Liu et al. 2014; Vásquez-Martínez et al. 2019). Interestingly, according to the physicochemical properties calculated by the free web-tool SwisADME, compound **24** will not be orally bioavailable, but compound **13** will be. Both of these compounds were, unfortunately, not lead-like based on the said parameters. (See “[In silico evaluation](#)” for the complete results and discussion).

Comparison of **29** (A_1K_i (*r*) = 6.1 μM) to **30–31** ([³H]DPCPX-specific binding > 20%) demonstrated the importance of the position of the Cl-atom on ring B for A_1 AR affinity; the $\text{C}2'$ (*ortho*) position (**29**) is preferred to the $\text{C}3'$ (*meta*) and/or $\text{C}4'$ (*para*) positions (**30–31**). Additionally, at the $\text{C}2'$ (*ortho*) position on ring B the more electronegative Cl-atom (**29**) is favoured over the less electronegative Br-atom (**26**). (It must be noted that compounds **26–27** and **30** retained some affinity against the A_1 AR based on the specific binding of less than 30%).

These trends were not observed with the $\text{C}3$ amino-substituted chalcone derivatives **37–41** (Table 3). Compound **29** paralleled to its counterpart **39** showed decreased A_1 AR affinity (**39**: [³H]DPCPX-specific binding = 26%); this may be credited to the combination of the NH_2 -group at position $\text{C}3$ on ring A and the Cl-atom at position $\text{C}2'$. Furthermore, $\text{C}2'$ (*ortho*) Br-group substitution on ring B led to

A_1 AR affinity below 10 μM ; for example, compound **37** (A_1K_i (*r*) = 7.1 μM) versus **39** ([³H]DPCPX-specific binding = 26%). The A_1 AR affinity was enhanced almost five-fold when the Br-atom was moved from the $\text{C}2'$ position (**37**) to the $\text{C}3'$ position (**38**) on ring B. The importance of the $\text{C}3$ NH_2 -group substitution on ring A to attain A_1 AR affinity was demonstrated by comparison of compound **38** to its unsubstituted counterpart **27** ([³H]DPCPX-specific binding = 28%). Compound **38** had a K_i value of 1.6 μM against the A_1 AR—the best of the evaluated compounds. Therefore, it may be said that the A_1 AR favours $\text{C}3$ NH_2 -group substitution on ring A in combination with $\text{C}3'$ Br-atom substitution on ring B; based on these chalcones (**15–41**). The SAR of the chalcone derivatives **27** and **29** and **37–39** are summarized in Fig. 6.

Interestingly, the $\text{C}3$ amino-substituted chalcones **37** ([³H]NECA-specific binding = 30%) and **39** ([³H]NECA-specific binding = 23%) with a $\text{C}2'$ substituent [either a Br- (**37**) or Cl-atom (**39**)] on ring B retained some affinity against the A_{2A} AR, unlike compounds **38** ([³H]NECA-specific binding = 75%), **40** ([³H]NECA-specific binding = 72%) and **41** ([³H]NECA-specific binding = 71%) with a $\text{C}3'$ substituent [either a Br- (**38**), Cl- (**40**) or F-atom (**41**)]. (Again, it must be noted that compounds **39–41** retained some affinity against the A_1 AR based on the radioligand-specific binding of less than 30%). The importance of not only the type of

Table 2 K_i values for the binding affinity of chalcone derivatives (**15–36**) against rat (*r*) A_1 and A_{2A} ARs


#	Ring A			Ring B					$K_i \pm \text{SEM}$ (μM) ^a [specific binding (%)] ^b	
	2	3	4	2'	3'	4'	5'	6'	rA_1^c vs [³ H]DPCPX ^e	rA_{2A}^d vs [³ H]NECA ^f
	R ¹	R ²	R ³	R ^{1'}	R ^{2'}	R ^{3'}	R ^{4'}	R ^{5'}		
Structural modification of ring A										
15	H	H	H	H	H	H	H	H	(35)	(79)
16	OH	H	H	H	H	H	H	H	(65)	(129)
17	H	H	OH	H	H	H	H	H	(56)	(83)
18	H	H	OCH ₃	H	H	H	H	H	(141)	(106)
19	H	H	Br	H	H	H	H	H	(117)	(117)
Structural modification of ring B										
20	H	H	H	H	OH	H	H	H	(32)	(40)
21	H	H	H	H	OCH ₃	H	H	H	(33)	(106)
22	H	H	H	H	H	OCH ₃	H	H	(45)	(78)
23	H	H	H	OCH ₃	H	OCH ₃	H	H	(30)	(50)
24	H	H	H	OCH ₃	H	OCH ₃	OCH ₃	H	5.3 ± 1	(28)
25	H	H	H	OCH ₃	H	OCH ₃	H	OCH ₃	(27)	(28)
26	H	H	H	Br	H	H	H	H	(24)	(50)
27	H	H	H	H	Br	H	H	H	(28)	(42)
28	H	H	H	H	H	Br	H	H	(110)	(91)
29	H	H	H	Cl	H	H	H	H	6.1 ± 1.1	(42)
30	H	H	H	H	Cl	H	H	H	(23)	(88)
31	H	H	H	H	Cl	Cl	H	H	(114)	(77)
32	H	H	H	H	H	F	H	H	(49)	(98)
33	H	H	H	H	H	CF ₃	H	H	(80)	(156)
34	H	H	H	H	CN	H	H	H	(52)	(155)
35	H	H	H	–	–	–	–	–	(55)	(75)
36	H	OCH ₃	H	–	–	–	–	–	(43)	(73)

^aAll K_i values were determined in triplicate and expressed as mean \pm standard error of the mean (SEM) in μM

^bSpecific binding (%) of the radioligand at a maximum tested concentration of 100 μM were determined in duplicate and expressed as the mean in %

^cRat receptors were used (rA_1 : rat whole brain membranes)

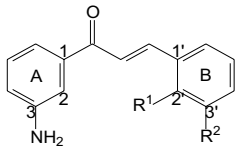
^dRat receptors were used (rA_{2A} : rat striatal membranes)

^e0.1 nM [³H]DPCPX

^f4 nM [³H]NECA

substituent, but also the position of the substituent on ring B is clear from these comparisons, for example, a compound with selective A_1 AR affinity may be obtained when a C3 NH₂-group substitution on ring A is combined with a C3' halogen (Br > Cl > F) substitution on ring B of the chalcone scaffold (e.g. **38**, **40–41**), whereas a C2' halogen-substituted ring B could yield a compound with dual A_1 and/or A_{2A} AR

affinity (**37** and **39**). Previously, it was found that a coplanar geometry between the two ring systems (namely, ring A and benzylidene ring B) in the flavonols (notably, chalcones may be considered open-chain flavonols) is not required for residual A_1 and/or A_{2A} AR affinity; however, the C2' position on ring B of compounds **37** and **39** was substituted (like the flavonol MRS 1067 with a planar geometry), and thus,

Table 3 K_i values for the binding affinity of chalcone derivatives (**37–41**) against rat (*r*) A_1 and A_{2A} ARs


#	Ring B		$K_i \pm \text{SEM}$ (μM) ^a [specific binding (%) ^b	
	2'	3'	rA_1 ^c vs [³ H]DPCPX ^e	rA_{2A} ^d vs [³ H]NECA ^f
	R ¹	R ²		
37	Br	H	7.1 ± 0.57^a	(30) ^b
38	H	Br	1.6 ± 0.02^a	(75) ^b
39	Cl	H	(26) ^b	(23) ^b
40	H	Cl	(30) ^b	(72) ^b
41	H	F	(26) ^b	(71) ^b

^aAll K_i values were determined in triplicate and expressed as mean \pm standard error of the mean (SEM) in μM

^bSpecific binding (%) of the radioligand at a maximum tested concentration of 100 μM were determined in duplicate and expressed as the mean in %

^cRat receptors were used (rA_1 : rat whole brain membranes)

^dRat receptors were used (rA_{2A} : rat striatal membranes)

^e0.1 nM [³H]DPCPX

^f4 nM [³H]NECA

there is likely also steric hindrance to free rotation of the benzylidene ring B of these compounds (**37** and **39**) (Karton et al. 1996). Notably, the structurally related 2-benzylidene-1-indanone **14** (Janse van Rensburg et al. 2019a) that is also C3' bromo-substituted on benzylidene ring B has selective A_{2A} AR affinity, unlike compound **38** (Fig. 7). Therefore, the benzylidene indanone scaffold with C4 hydroxy-substitution on ring A may be essential to selective A_{2A} AR affinity when compared to the C3 amino-substituted chalcone scaffold. Compound **14** is structurally related to chromone hits with selective A_{2A} AR affinity based on virtual screening, and perhaps, the conformation of these chromones binding to the A_{2A} AR is similar to that of compound **14**—leading to selectivity of the A_{2A} AR versus the A_1 AR (Langmead et al. 2012).

Additionally, SAR demonstrated the importance of, among other, the phenol functionality in triazine virtual screening hits for selective A_{2A} AR affinity; possibly due to the hydrogen bonding between the phenol functionality and Asn253^{6.55} (Langmead et al. 2012). This key hydrogen bonding residue (Asn253^{6.55}) is situated centrally and capable of high-quality interactions with diverse heterocyclic compounds (Langmead et al. 2012). Therefore, the phenol

functionality (present in compound **14**) may also be responsible for the selectivity of the said compound (as seen with the triazine virtual screening hits).

As seen in Table 4 the Schiff base containing compounds **42–47** showed poor A_1 and A_{2A} AR affinity. The best radioligand-specific binding at a concentration of 100 μM against A_1 and/or A_{2A} AR was demonstrated by compounds **45** and **47**; displacing more than 50% of the radioligand at A_1 (**45** and **47**) and A_{2A} (**45**) ARs. Comparison of **44** to **45** showed that the inclusion of a bromine atom at position C3' (**44**), rather than a hydrogen atom (**45**), in combination with C2'–OH and C5'–Cl substitution on ring B was detrimental to both A_1 and A_{2A} AR affinity as the radioligand-specific binding increased more than twofold. The A_1 AR seemed to be more tolerable toward the said substitution. Schiff base or imine derivatives are important synthetic intermediates (Furniss et al. 1989); therefore, the synthesised and evaluated compounds **42–47** may be of use in future studies.

GTP shift assays

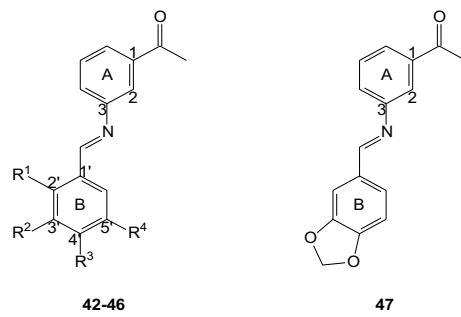
The type of binding affinity that test compounds **24** and **38** exhibited at the rat A_1 AR was determined via a GTP shift assay, as described previously (Lohse et al. 1987; Van der Walt and Terre'Blanche 2015; Van der Werden et al. 1995). GTP shifts were calculated by dividing the K_i values of compounds reported in the presence of GTP by the K_i values obtained in the absence of GTP and the results are summarized in Table 5.

Test compounds **24** and **38** were selected as they possessed the highest A_1 AR affinity in the three respective series (Tables 2, 3, 4). The results suggested that compounds **24** and **38** acted as A_1 AR antagonists, as the binding curves in the presence of GTP were almost unaffected and the calculated GTP shifts were approximately 1 (Table 5; Fig. 8) (Van der Werden et al. 1995; Gütschow et al. 2012). On account of the structural similarity of the test compounds (**15–23**, **25–36**, **37** and **39–41**), it may be supposed that these chalcone derivatives were all A_1 AR antagonists.

In silico evaluation

The physiochemical, pharmacokinetic as well as drug-likeness and medicinal chemistry friendliness of compounds **24**, **29**, **37** and **38** (the only test compounds with selective A_1 AR affinity) were computed via SwissADME and these results are summarized in Tables 6, 7 and 8, respectively.

The bioavailability radar (Fig. 9) gave a first glance at the drug-likeness of these compounds; compounds **24**, **29**, **37** and **38** fall within the optimal range for the parameters lipophilicity, size, polarity, solubility and flexibility (see Table 6), except for saturation ($C_{sp^3} > 0.25$). The fraction of carbon atoms in the sp^3 hybridization of compounds **24**

Table 4 K_i values for the binding affinity of Schiff base derivatives (**42–47**) against rat (r) A_1 and A_{2A} ARs


#	Ring B				$K_i \pm \text{SEM}$ (μM) ^a [specific binding (%) ^b]	
	2'	3'	4'	5'	rA_1 ^c vs [³ H]DPCPX ^e	rA_{2A} ^d vs [³ H]NECA ^f
	R ^{1'}	R ^{2'}	R ^{3'}	R ^{4'}		
42	OH	H	OCH ₃	H	(91) ^b	(197) ^b
43	OH	H	H	OCH ₃	(70) ^b	(75) ^b
44	OH	Br	H	Cl	(101) ^b	(95) ^b
45	OH	H	H	Cl	(44) ^b	(43) ^b
46	OH	H	N(CH ₂ CH ₃) ₂	H	(74) ^b	(69) ^b
47	–	–	–	–	(47) ^b	(66) ^b

^aAll K_i values were determined in triplicate and expressed as mean \pm standard error of the mean (SEM) in μM

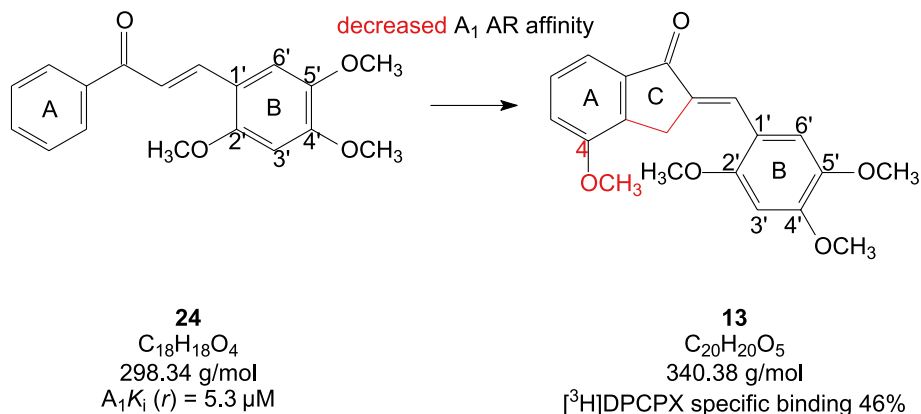
^bSpecific binding (%) of the radioligand at a maximum tested concentration of 100 μM were determined in duplicate and expressed as the mean in %

^cRat receptors were used (rA_1 : rat whole brain membranes)

^dRat receptors were used (rA_{2A} : rat striatal membranes)

^e0.1 nM [³H]DPCPX

^f4 nM [³H]NECA

Fig. 5 The structure–affinity relationships (SAR) of compound **24** versus **13**

(0.17), **29** (0), **37** (0) and **38** (0) were smaller than 0.25 and, thus, out of range. Consequently, compounds **24**, **29**, **37** and **38** were predicted not orally bioavailable.

The qualitative solubility classes of compounds **24**, **29**, **37** and **38** were moderately soluble to soluble in water [the predicted values are the decimal logarithm of the molar solubility in water (logS)]. This was encouraging given

the poor solubility of most chalcone-based compounds [most probably the reason for poor in vivo efficacy in pre-clinical studies (Zhuang et al. 2017)]. Seeing as solubility influences GI absorption (Ottaviani et al. 2010), a soluble molecule will most probably facilitate drug development (Ritchie et al. 2013).

Fig. 6 The structure–affinity relationships (SAR) of compounds **27** and **29** and **37–39**; highlighting the importance of C3 NH₂-substitution on ring A in combination with C3' (*meta*) Br substitution on ring B for selective *r*A₁ AR affinity

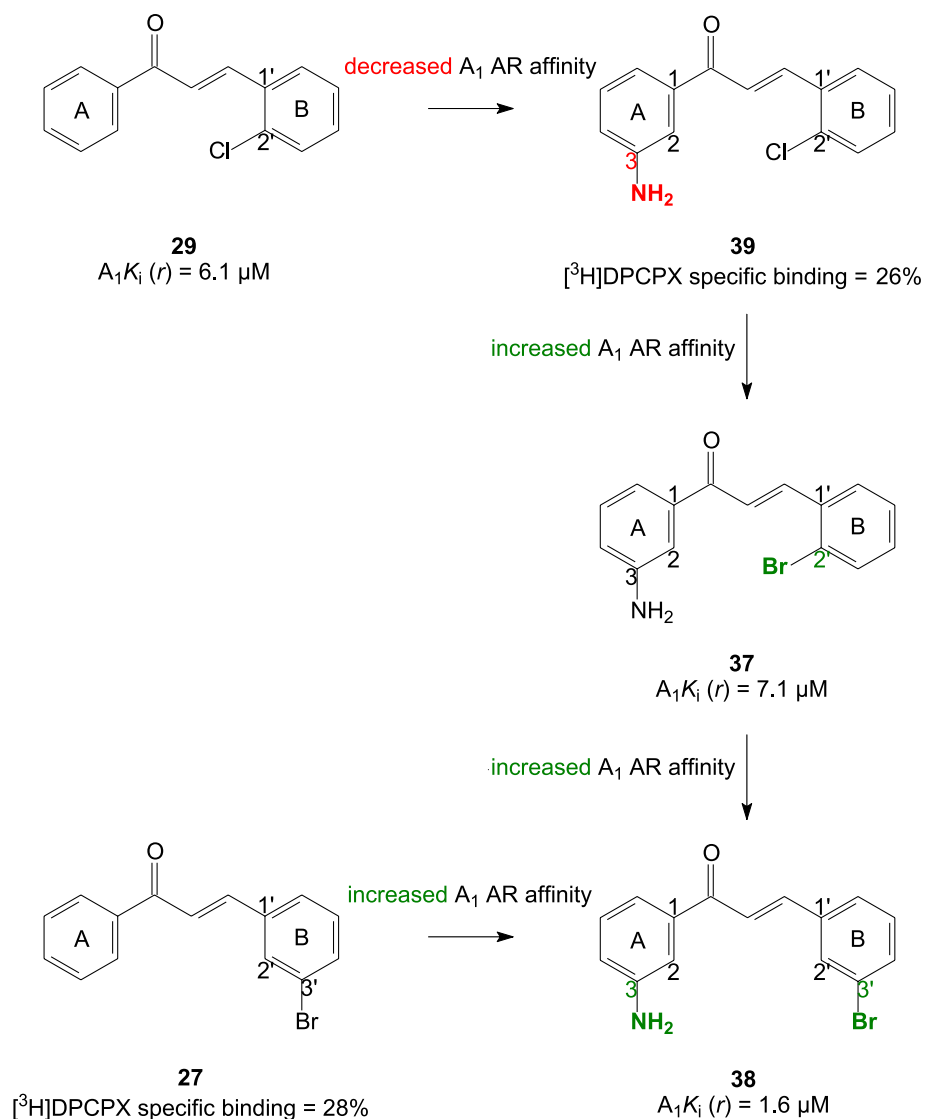
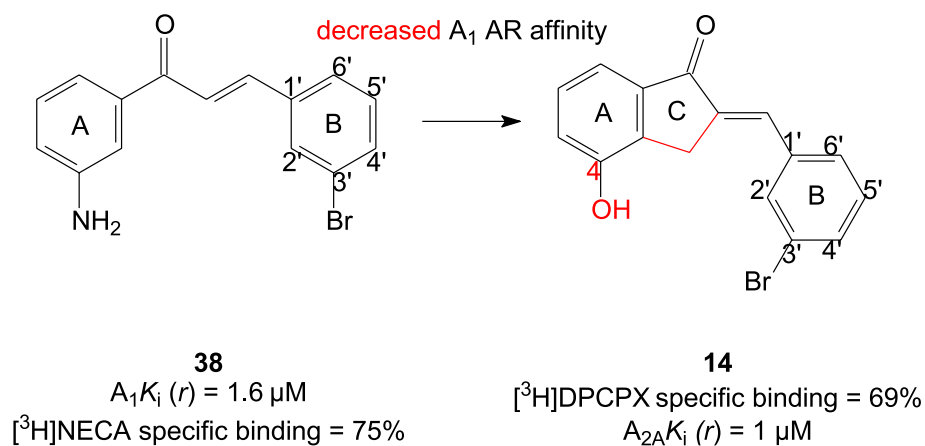


Fig. 7 The structure–affinity relationships (SAR) of compound **38** versus **14**



The BOILED-Egg model (Fig. 10) predicted passive human gastrointestinal absorption (HIA) and blood–brain-barrier (BBB) permeation as a function of the position of the

compound in the WLOGP-versus-TPSA referential (Daina and Zoete 2016). Compounds **24**, **29**, **37** and **38** were predicted to have high GI absorption and permeate the BBB

Table 5 A_1K_i values (in the absence and presence of GTP) and calculated GTP shifts of **24** and **38**

#	$K_i \pm \text{SEM} (\mu\text{M})^a$		GTP shift ^e
	rA_1^b vs [^3H]DPCPX ^c	$rA_1^b + \text{GTP}^d$ vs [^3H]DPCPX ^c	
24	5.3 ± 1^a	7.8 ± 0.68	1.5
38	1.6 ± 0.02^a	1.7 ± 1.3	1.1

^a K_i values were determined in triplicate and expressed as mean \pm standard error of the mean (SEM) in μM

^bRat receptors were used (A_1 : rat whole brain membranes)

^c0.1 nM [^3H]DPCPX

^dAddition of 100 μM GTP to A_1 AR radioligand binding assay

^eGTP shift calculated by dividing K_i value in the presence of 100 μM GTP by K_i value in the absence of 100 μM GTP

(Table 7). Additionally, these compounds were not substrates for the permeability glycoprotein (Pgp) responsible for efflux through biological membranes, for instance from the gastrointestinal wall to the lumen or from the brain (Montanari and Ecker 2015). Pgp also protects the CNS from xenobiotics (Szakács et al. 2008).

The interaction of a compound with cytochromes P450 (CYP) is important; seeing as these isoenzymes modulate drug elimination through metabolic transformation (Testa and Kraemer 2007); probably causing pharmacokinetics-related drug–drug interactions (Hollenberg 2002; Huang et al. 2008), leading to adverse or even toxic effects due to the lower clearance and accumulation of the drug or its metabolites (Kirchmair et al. 2015). Compounds **24**, **29**, **37** and **38** were predicted to inhibit the major CYP isoforms (CYP12, CYP2C19, CYP2C9, CYP2D6 and CYP3A4),

with the exception of **24** and/or **37–38** that did not inhibit CYP2D6 (**29** and **37–38**) and CYP3A4 (**29**).

The drug-likeness of compounds **24**, **29**, **37** and **38** was assessed by various rule-based filters (Egan et al. 2000; Ghose et al. 1999; Lipinski et al. 1997; Muegge et al. 2001; Veber et al. 2002) (Table 8). Compound **29** violated a rule-based filter from Muegge (Muegge et al. 2001); namely that a compound should contain more than one heteroatom and the only atom other than carbon and hydrogen that **29** contained was a chloro atom. Additionally, compounds **24**, **29**, **37** and **38** all had a bioavailability score of 0.55 (the probability that a compound will have > 10% bioavailability in rat or measurable Caco-2 permeability) (Martin 2005).

The medicinal chemistry friendliness of compounds **24**, **29**, **37** and **38** was assessed by the identification of potentially problematic fragments; first, pan assay interference compounds (PAINS) (Baell and Holloway 2010) and, second, structural alerts (Brenk et al. 2008). Compounds **24**, **29**, **37** and **38** contained no PAINS; however, Brenk violations were present (Table 8). All these compounds contained an α,β -unsaturated carbonyl system perceived as a potential Michael acceptor. Additionally, compounds **37–38** contained a potentially unwanted aniline group; as aniline groups are perhaps inclined toward problems with genetic toxicity (Clayson 1981).

As compounds **24**, **29**, **37** and **38** did not have pronounced affinity toward the A_1 AR, the present structures need to be optimised, and here, lead-likeness [a molecular entity suitable for optimization, most probably increasing size and lipophilicity (Hann and Keserü 2012)] plays a role (Teague et al. 1999). Accordingly, compounds **24**, **37** and **38** (but not compound **29**; due to molecular weight value

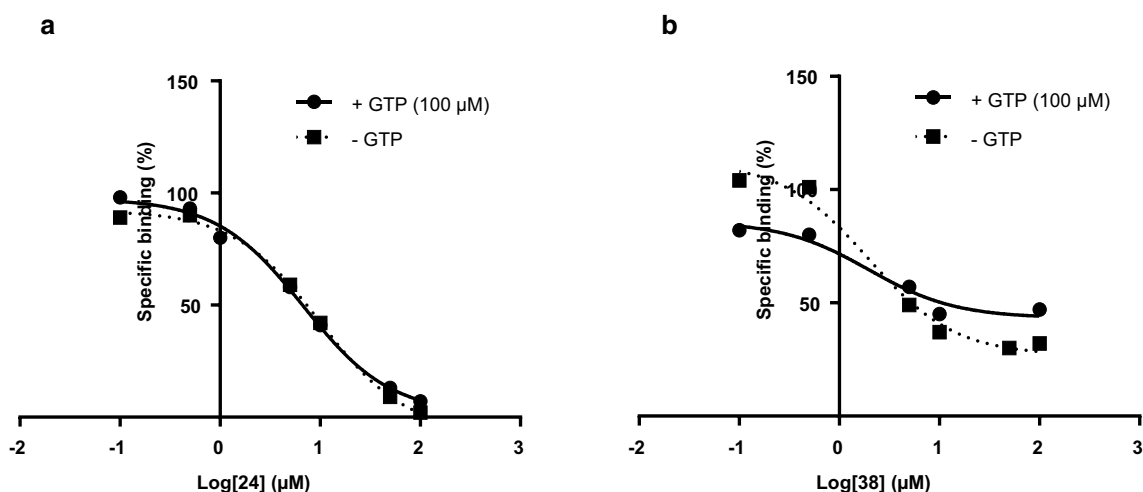


Fig. 8 The binding curves of compounds **24** (a) and **38** (b) are examples of A_1 AR antagonistic action determined via a GTP shift assay performed in triplicate (with and without 100 μM GTP) using rat

whole brain membranes expressing A_1 ARs with [^3H]DPCPX as radioligand. Calculated GTP shift of: 1.5 (**24**) and 1.1 (**38**)

Table 6 Physicochemical properties of compounds **24**, **29**, **37** and **38**

#	Physicochemical properties							Lipophilicity		Water solubility	
	Molecular formula	Molecular weight (g/mol)	Fraction C _{sp3}	Num. rotatable bonds	Num. H-bond acceptors	Num. H-bond donors	Molar refractivity	TPSA (Å ²)	Consensus log $P_{o/w}$	Consensus log S	
24	C ₁₈ H ₁₈ O ₄	298.33	0.17	6	4	0	85.72	44.76	3.36	-4.51	
29	C ₁₅ H ₁₃ O	242.70	0	3	1	0	71.26	17.07	3.98	-4.89	
37	C ₁₅ H ₁₂ BrNO	302.17	0	3	1	1	78.35	43.09	3.46	-4.69	
38	C ₁₅ H ₁₂ BrNO	302.17	0	3	1	1	78.35	43.09	3.53	-4.86	

smaller than 250 g/mol and consensus log $P_{o/w}$ value larger than 3.5) may be considered lead-like (Tables 6, 8).

Therefore, the optimization of the physicochemical properties of chalcones and, thus, the pharmacokinetic properties as well as drug-likeness and medicinal chemistry friendliness is of great importance for medicinal chemistry research on chalcone-based compounds.

Experimental

Chemistry

Materials

Unless otherwise noted, all starting materials and solvents were purchased from commercial vendors and used without further purification. Thin layer chromatography on TLC silica gel 60 F₂₅₄ aluminium sheets from Merck was used to monitor reaction progress. Melting points were determined by means of differential scanning calorimetry (DSC) with a Mettler DSC 3 Star System (Mettler Toledo, Greifensee, Switzerland). Proton (¹H) and carbon (¹³C) nuclear magnetic resonance (NMR) spectra were recorded on a Bruker Avance III 600 spectrometer at frequencies of 600 and 151 MHz, respectively, using either CDCl₃ or DMSO-d₆ as solvent and TMS as reference. Chemical shifts were reported in parts per million (ppm) in relation to the solvent peak (CDCl₃: residual CH at 7.26 ppm and DMSO-d₆: residual CH₃ at 2.50 ppm for ¹H NMR). Spin multiplicities were indicated as follows: singlet (s), doublet (d), triplet (t), quartet (q), doublet of doublets (dd), triplet of doublets (td), double doublet (ddd) and multiplet (m). Coupling constant (*J*) values were reported in Hertz (Hz). High-resolution mass spectra (HRMS) were recorded on a Bruker micrOTOF-Q II mass spectrometer in atmospheric chemical ionisation (APCI) mode. High-performance liquid chromatography (HPLC) analyses were done on an Agilent 1100 HPLC system.

Synthesis of 15–36

(2E)-1,3-Diphenylprop-2-en-1-one (15) A solution of acetophenone (0.50 g, 4.16 mmol) and benzaldehyde (0.44 g, 4.16 mmol) in EtOH (5 mL) was mechanically stirred at room temperature for approximately 5 min before the dropwise addition of KOH (10% (w/v) aqueous solution, 5 mL). The subsequent reaction mixture was mechanically stirred at room temperature and continuously monitored by TLC. Upon completion, the reaction mixture was quenched with crushed ice (15 g) and acidified to pH 2 with HCl (32 wt. % in H₂O, FCC). The subsequent precipitate was collected by vacuum filtration, dried (30 °C) and recrystallized from

Table 7 Pharmacokinetic properties of compounds **24**, **29**, **37** and **38**

#	Pharmacokinetic properties							
	GI absorption	BBB permeation	Pgp substrate	CYP12 inhibitor	CYP2C19 inhibitor	CYP2C9 inhibitor	CYP2D6 inhibitor	CYP3A4 inhibitor
24	High	Yes	No	Yes	Yes	Yes	Yes	Yes
29	High	Yes	No	Yes	Yes	Yes	No	No
37	High	Yes	No	Yes	Yes	Yes	No	Yes
38	High	Yes	No	Yes	Yes	Yes	No	Yes

Table 8 Drug-likeness and medicinal chemistry friendliness of compounds **24**, **29**, **37** and **38**

#	Drug-likeness					Lead-likeness		
	Num. violations							
	Lipinski ^a	Ghose ^b	Veber ^c	Egan ^d	Muegge ^e	PAINS ^f	Brenk ^g	Teague ^h
24	0	0	0	0	0	0	1	0
29	0	0	0	0	1	0	1	2
37	0	0	0	0	0	0	2	0
38	0	0	0	0	0	0	2	0

^aLipinski: MW < 500, MLOGP < 4.15, N or O < 10, NH or OH < 5 (Lipinski et al. 1997)

^bGhose: 160 < MW < 480, -04 < WLOGP < 5.6, 40 < MR < 130, 20 < atoms < 70 (Ghose et al. 1999)

^cVeber: Num. rotatable bonds < 10, TPSA < 140 (Veber et al. 2002)

^dEgan: WLOGP < 5.88, TPSA < 131.6 (Egan et al. 2000)

^eMuegge: 200 < MW < 600, -2 < XLOGP < 5, TPSA < 150, num. rings < 7, num. carbon > 4, num. heteroatoms > 1, num. rotatable bonds < 15, num. H-bond acceptors < 10, num. H-bond donors < 5 (Muegge et al. 2001)

^fPan assay interference compounds (PAINS) implemented from Baell and Holloway (2010)

^gStructural alert implemented from Brenk et al. (2008)

^hTeague: 250 < MW < 350, num. rotatable bonds < 7, XLOGP3 < 3.5 (Teague et al. 1999)

EtOH to yield the title compound **15** as light yellow crystals (0.43 g, 49%): mp: 57.87 °C (EtOH); ¹H NMR (600 MHz, DMSO) δ 8.16 (d, *J* = 7.7 Hz, 2H), 7.95 (d, *J* = 15.6 Hz, 1H), 7.89 (d, *J* = 4.8 Hz, 2H), 7.76 (d, *J* = 15.6 Hz, 1H), 7.68 (t, *J* = 7.3 Hz, 1H), 7.58 (t, *J* = 7.5 Hz, 2H), 7.46 (d, *J* = 4.4 Hz, 3H) (Xie et al. 2017). Purity (HPLC): 99.8%.

(2E)-1-(2-Hydroxyphenyl)-3-phenylprop-2-en-1-one (16) Prepared as for **15** from 2'-hydroxyacetophenone (0.50 g, 3.67 mmol) and benzaldehyde (0.39 g, 3.67 mmol) to yield the title compound **16** as dark yellow crystals (0.05 g, 6%): mp: 87.21 °C (EtOH); ¹H NMR (600 MHz, CDCl₃) δ 12.82 (s, 1H), 7.97–7.90 (m, 2H), 7.71–7.64 (m, 3H), 7.51 (t, *J* = 7.7 Hz, 1H), 7.45 (d, *J* = 2.6 Hz, 3H), 7.04 (d, *J* = 8.3 Hz, 1H), 6.95 (t, *J* = 7.5 Hz, 1H) (Xie et al. 2017). Purity (HPLC): 99%.

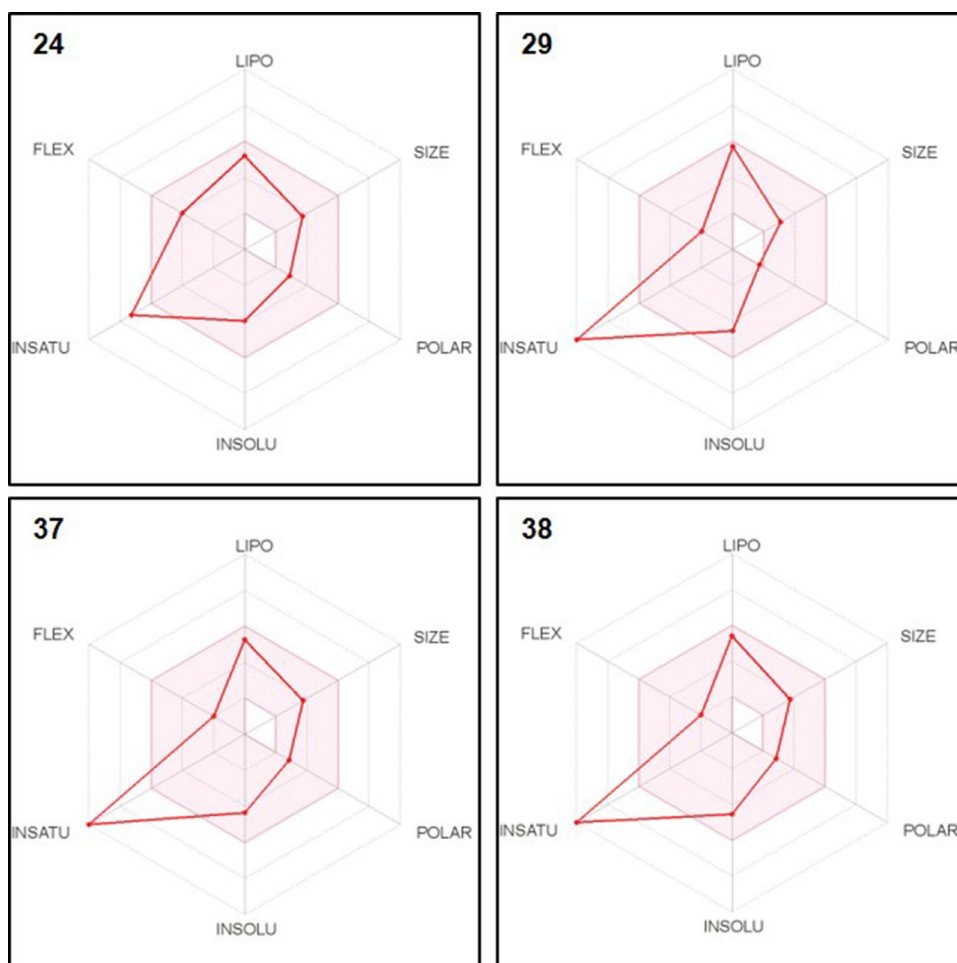
(2E)-1-(4-Hydroxyphenyl)-3-phenylprop-2-en-1-one (17) Prepared as for **15** from 4'-hydroxyacetophenone (0.50 g, 3.67 mmol) and benzaldehyde (0.39 g, 3.67 mmol) to yield the title compound **17** as beige crystals (0.15 g, 18%): mp: 171.29 °C (EtOH); ¹H NMR (600 MHz,

DMSO) δ 10.46 (d, *J* = 7.9 Hz, 1H), 8.10–8.04 (m, 2H), 7.90 (d, *J* = 15.6 Hz, 1H), 7.86 (dd, *J* = 7.5, 1.7 Hz, 2H), 7.68 (d, *J* = 15.6 Hz, 1H), 7.45 (d, *J* = 6.9 Hz, 3H), 6.93–6.89 (m, 2H) (Xie et al. 2017). Purity (HPLC): 98.9%.

(2E)-1-(4-Methoxyphenyl)-3-phenylprop-2-en-1-one (18) Prepared as for **15** from 4'-methoxyacetophenone (0.50 g, 3.33 mmol) and benzaldehyde (0.35 g, 3.33 mmol) to yield the title compound **18** as white crystals (0.79 g, 52%): mp: 105.91 °C (EtOH); ¹H NMR (600 MHz, DMSO) δ 8.17 (d, *J* = 7.7 Hz, 2H), 7.94 (d, *J* = 15.6 Hz, 1H), 7.88 (d, *J* = 6.8 Hz, 2H), 7.71 (d, *J* = 15.6 Hz, 1H), 7.45 (d, *J* = 5.5 Hz, 3H), 7.09 (d, *J* = 7.7 Hz, 2H), 3.87 (s, 3H) (Zhang et al. 2015). Purity (HPLC): 97.2%.

(2E)-1-(4-Bromophenyl)-3-phenylprop-2-en-1-one (19) Prepared as for **15** from 4'-bromoacetophenone (0.50 g, 2.51 mmol) and benzaldehyde (0.27 g, 2.51 mmol) to yield the title compound **19** as light yellow crystals (0.72 g, 63%): mp: 103.26 °C (EtOH); ¹H NMR (600 MHz, CDCl₃) δ 7.92–7.87 (m, 2H), 7.82 (d, *J* = 15.7 Hz, 1H),

Fig. 9 The pink area represents the optimal range for lipophilicity (LIPO: $-0.7 < \text{XLOGP3} < +5.0$), size (SIZE: $150 < \text{MW} < 500$), polarity (POLAR: $20 < \text{TPSA} < 130$), solubility (INSOLU: $\log S < 6$), saturation (INSATU: fraction $\text{Csp}^3 > 0.25$) and flexibility (FLEX: num. rotatable bonds < 9). The red lines represent the said parameters of compounds **24**, **29**, **37** and **38**. The red lines must fall completely within the pink area for a compound to be considered drug-like; therefore, compounds **24**, **29**, **37** and **38** are predicted not orally bioavailable



7.69–7.60 (m, 4H), 7.48 (d, $J=15.7$ Hz, 1H), 7.44–7.40 (m, 3H) (Zhou et al. 2016). Purity (HPLC): 98%.

(2E)-3-(3-Hydroxyphenyl)-1-phenylprop-2-en-1-one (20) Prepared as for **15** from acetophenone (0.50 g, 4.16 mmol) and 3-hydroxybenzaldehyde (0.51 g, 4.16 mmol) to yield the title compound **20** as light yellow crystals (0.51 g, 55%): mp: 163.81 °C (EtOH); ^1H NMR (600 MHz, DMSO) δ 9.63 (s, 1H), 8.17–8.09 (m, 2H), 7.83 (d, $J=15.6$ Hz, 1H), 7.69–7.63 (m, 2H), 7.57 (t, $J=7.7$ Hz, 2H), 7.31 (d, $J=7.7$ Hz, 1H), 7.26 (t, $J=7.8$ Hz, 1H), 7.23 (s, 1H), 6.88 (dd, $J=7.9$, 1.7 Hz, 1H) (Xie et al. 2017). Purity (HPLC): 99.9%.

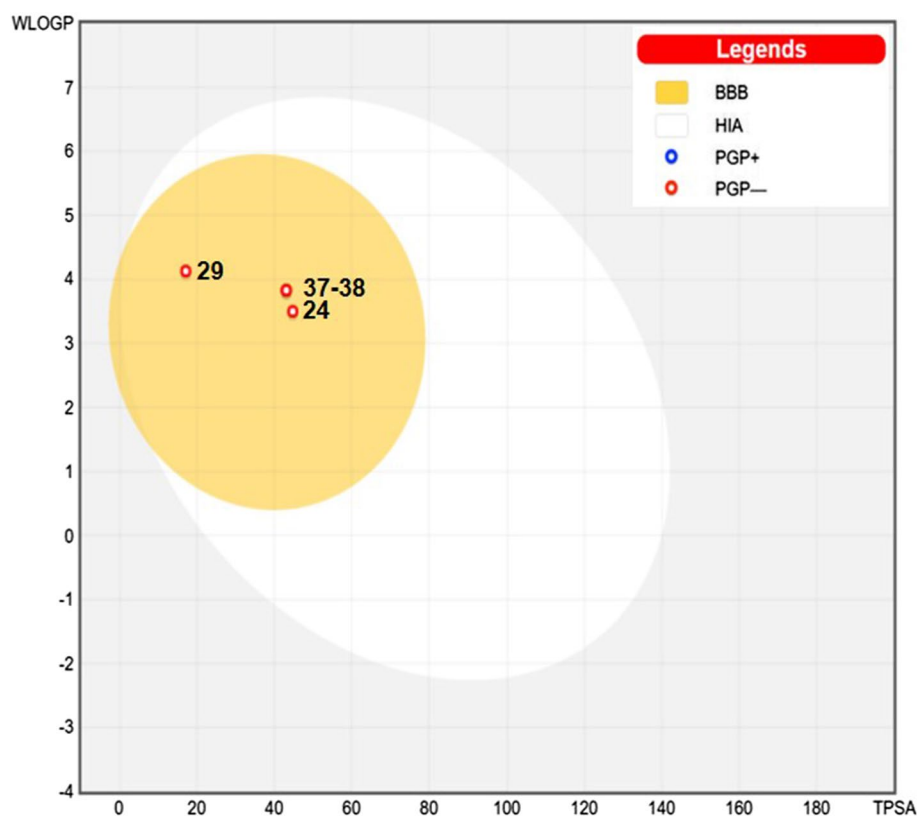
(2E)-3-(3-Methoxyphenyl)-1-phenylprop-2-en-1-one (21) Prepared as for **15** from acetophenone (0.50 g, 4.16 mmol) and 3-methoxybenzaldehyde (0.57 g, 4.16 mmol) to yield the title compound **21** as dark yellow crystals (0.19 g, 19%): mp: 60.43 °C (EtOH); ^1H NMR (600 MHz, CDCl_3) δ 8.14–8.10 (m, 2H), 7.88 (d, $J=15.7$ Hz, 1H), 7.69 (t, $J=7.4$ Hz, 1H), 7.64–7.58 (m, 3H), 7.44 (t, $J=7.9$ Hz, 1H), 7.38–7.32 (m, 1H), 7.26 (d,

$J=1.7$ Hz, 1H), 7.07 (dd, $J=8.2$, 2.4 Hz, 1H), 3.96 (s, 3H) (Unoh et al. 2013). Purity (HPLC): 98.2%.

(2E)-3-(4-Methoxyphenyl)-1-phenylprop-2-en-1-one (22) Prepared as for **15** from acetophenone (0.50 g, 4.16 mmol) and 4-methoxybenzaldehyde (0.57 g, 4.16 mmol) to yield the title compound **22** as light yellow crystals (0.06 g, 6%): mp: 72.02 °C (EtOH); ^1H NMR (600 MHz, DMSO) δ 8.17–8.08 (m, 2H), 7.88–7.83 (m, 2H), 7.80 (d, $J=15.6$ Hz, 1H), 7.72 (d, $J=15.6$ Hz, 1H), 7.66 (t, $J=7.4$ Hz, 1H), 7.57 (t, $J=7.7$ Hz, 2H), 7.06–6.97 (m, 2H), 3.83 (s, 3H) (Zhang et al. 2015). Purity (HPLC): 100%.

(2E)-3-(2,4-Dimethoxyphenyl)-1-phenylprop-2-en-1-one (23) Prepared as for **15** from acetophenone (0.50 g, 4.16 mmol) and 2,4-dimethoxybenzaldehyde (0.69 g, 4.16 mmol) to yield the title compound **23** as dark yellow crystals (0.18 g, 16%): mp: 69.63 °C (EtOH); ^1H NMR (600 MHz, DMSO) δ 8.08 (d, $J=7.5$ Hz, 2H), 7.99 (d, $J=15.7$ Hz, 1H), 7.91 (d, $J=8.6$ Hz, 1H), 7.74 (d, $J=15.7$ Hz, 1H), 7.64 (t, $J=7.3$ Hz, 1H), 7.56 (t, $J=7.6$ Hz,

Fig. 10 Compounds **24**, **29**, **37** and **38**, which are not a substrate for Pgp (PGP-), is represented by the red circles in the yellow region. The white region is for high probability of passive absorption by the gastrointestinal tract (HIA), and the yellow region (yolk) is for high probability of brain penetration (BBB). White and yellow (yolk) regions are not mutually exclusive



2H), 6.67–6.60 (m, 2H), 3.90 (s, 3H), 3.84 (s, 3H) (Suwito et al. 2014). Purity (HPLC): 94.8%.

(2E)-1-Phenyl-3-(2,4,5-trimethoxyphenyl)prop-2-en-1-one (24) Prepared as for **15** from acetophenone (0.50 g, 4.16 mmol) and 2,4,5-trimethoxybenzaldehyde (0.82 g, 4.16 mmol) to yield the title compound **24** as dark yellow crystals (0.95 g, 79%): mp: 102.97 °C (EtOH); ¹H NMR (600 MHz, CDCl₃) δ 8.09 (d, *J* = 15.8 Hz, 1H), 8.03–7.97 (m, 2H), 7.55 (t, *J* = 7.3 Hz, 1H), 7.47 (dd, *J* = 20.6, 11.8 Hz, 3H), 7.13 (s, 1H), 6.52 (s, 1H), 3.94 (s, 3H), 3.90 (s, 6H) (Shenvi et al. 2013). Purity (HPLC): 97.6%.

(2E)-1-Phenyl-3-(2,4,6-trimethoxyphenyl)prop-2-en-1-one (25) Prepared as for **15** from acetophenone (0.50 g, 4.16 mmol) and 2,4,6-trimethoxybenzaldehyde (0.82 g, 4.16 mmol) to yield the title compound **25** as bright yellow crystals (0.43 g, 35%): mp: 109.17 °C (EtOH); ¹H NMR (600 MHz, CDCl₃) δ 8.26 (d, *J* = 15.9 Hz, 1H), 8.03–7.98 (m, 2H), 7.88 (d, *J* = 15.9 Hz, 1H), 7.53 (t, *J* = 7.3 Hz, 1H), 7.47 (t, *J* = 7.5 Hz, 2H), 6.14 (s, 2H), 3.90 (s, 6H), 3.86 (s, 3H) (Sawle et al. 2008). Purity (HPLC): 88%.

(2E)-3-(2-Bromophenyl)-1-phenylprop-2-en-1-one (26) Prepared as for **15** from acetophenone (0.50 g, 4.16 mmol) and 2-bromobenzaldehyde (0.77 g, 4.16 mmol) to yield the title compound **26** as dark yellow crystals

(0.90 g, 75%): mp: 47.76 °C (EtOH); ¹H NMR (600 MHz, DMSO) δ 8.24–8.12 (m, 3H), 8.01 (d, *J* = 15.5 Hz, 1H), 7.95 (d, *J* = 15.5 Hz, 1H), 7.75 (dd, *J* = 8.0, 0.9 Hz, 1H), 7.69 (t, *J* = 7.4 Hz, 1H), 7.59 (t, *J* = 7.7 Hz, 2H), 7.50 (t, *J* = 7.5 Hz, 1H), 7.40 (td, *J* = 7.9, 1.6 Hz, 1H) (Wu et al. 2017). Purity (HPLC): 97.1%.

(2E)-3-(3-Bromophenyl)-1-phenylprop-2-en-1-one (27) Prepared as for **15** from acetophenone (0.50 g, 4.16 mmol) and 3-bromobenzaldehyde (0.77 g, 4.16 mmol) to yield the title compound **27** as light yellow crystals (0.62 g, 52%): mp: 84.50 °C (EtOH); ¹H NMR (600 MHz, DMSO) δ 8.24–8.16 (m, 3H), 8.03 (d, *J* = 15.6 Hz, 1H), 7.87 (d, *J* = 7.8 Hz, 1H), 7.74–7.62 (m, 3H), 7.58 (dd, *J* = 10.7, 4.7 Hz, 2H), 7.42 (t, *J* = 7.8 Hz, 1H) (Wang et al. 2019). Purity (HPLC): 86.5%.

(2E)-3-(4-Bromophenyl)-1-phenylprop-2-en-1-one (28) Prepared as for **15** from acetophenone (0.50 g, 4.16 mmol) and 4-bromobenzaldehyde (0.77 g, 4.16 mmol) to yield the title compound **28** as light yellow crystals (0.58 g, 49%): mp: 119.66 °C (EtOH); ¹H NMR (600 MHz, DMSO) δ 8.19–8.12 (m, 2H), 7.98 (d, *J* = 15.7 Hz, 1H), 7.87 (d, *J* = 8.5 Hz, 2H), 7.72 (d, *J* = 15.7 Hz, 1H), 7.69–7.64 (m, 3H), 7.58 (t, *J* = 7.7 Hz, 2H) (Wu et al. 2017). Purity (HPLC): 98.3%.

(2E)-3-(2-Chlorophenyl)-1-phenylprop-2-en-1-one (29) Prepared as for **15** from acetophenone (0.50 g, 4.16 mmol) and 2-chlorobenzaldehyde (0.58 g, 4.16 mmol) to yield the title compound **29** as light yellow crystals (0.32 g, 32%): mp: 50.30 °C (EtOH); ¹H NMR (600 MHz, DMSO) δ 8.23 (dd, *J* = 7.5, 1.9 Hz, 1H), 8.20–8.15 (m, 2H), 8.03 (q, *J* = 15.6 Hz, 2H), 7.72–7.66 (m, 1H), 7.62–7.55 (m, 3H), 7.52–7.43 (m, 2H) (Wu et al. 2017). Purity (HPLC): 97.5%.

(2E)-3-(3-Chlorophenyl)-1-phenylprop-2-en-1-one (30) Prepared as for **15** from acetophenone (0.50 g, 4.16 mmol) and 3-chlorobenzaldehyde (0.58 g, 4.16 mmol) to yield the title compound **30** as light yellow crystals (0.32 g, 32%): mp: 75.30 °C (EtOH); ¹H NMR (600 MHz, DMSO) δ 8.19 (d, *J* = 7.3 Hz, 2H), 8.09 (s, 1H), 8.04 (d, *J* = 15.7 Hz, 1H), 7.83 (d, *J* = 7.2 Hz, 1H), 7.73 (d, *J* = 15.7 Hz, 1H), 7.69 (t, *J* = 7.4 Hz, 1H), 7.58 (t, *J* = 7.7 Hz, 2H), 7.53–7.46 (m, 2H) (Robinson et al. 2015). Purity (HPLC): 96%.

(2E)-3-(3,4-Dichlorophenyl)-1-phenylprop-2-en-1-one (31) Prepared as for **15** from acetophenone (0.50 g, 4.16 mmol) and 3,4-dichlorobenzaldehyde (0.73 g, 4.16 mmol) to yield the title compound **31** as light yellow crystals (0.35 g, 30%): mp: 108.62 °C (EtOH); ¹H NMR (600 MHz, DMSO) δ 8.30 (d, *J* = 2.0 Hz, 1H), 8.21–8.17 (m, 2H), 8.07 (d, *J* = 15.7 Hz, 1H), 7.89 (dd, *J* = 8.4, 1.9 Hz, 1H), 7.75–7.66 (m, 3H), 7.59 (t, *J* = 7.7 Hz, 2H) (Choi et al. 2016). Purity (HPLC): 95.9%.

(2E)-3-(4-Fluorophenyl)-1-phenylprop-2-en-1-one (32) Prepared as for **15** from acetophenone (0.50 g, 4.16 mmol) and 4-fluorobenzaldehyde (0.52 g, 4.16 mmol) to yield the title compound **32** as light yellow crystals (0.32 g, 34%): mp: 86.71 °C (EtOH); ¹H NMR (600 MHz, DMSO) δ 8.15 (dd, *J* = 8.2, 1.1 Hz, 2H), 8.03–7.94 (m, 2H), 7.91 (d, *J* = 15.6 Hz, 1H), 7.75 (d, *J* = 15.7 Hz, 1H), 7.70–7.64 (m, 1H), 7.57 (dd, *J* = 10.7, 4.7 Hz, 2H), 7.34–7.26 (m, 2H) (Stroba et al. 2009). Purity (HPLC): 100%.

(2E)-1-Phenyl-3-[4-(trifluoromethyl)phenyl]prop-2-en-1-one (33) Prepared as for **15** from acetophenone (0.50 g, 4.16 mmol) and 4-(trifluoromethyl)benzaldehyde (0.72 g, 4.16 mmol) to yield the title compound **33** as light yellow crystals (0.41 g, 36%): mp: 126.59 °C (EtOH); ¹H NMR (600 MHz, DMSO) δ 8.20–8.16 (m, 2H), 8.11 (dd, *J* = 21.5, 11.9 Hz, 3H), 7.81 (dd, *J* = 11.9, 8.8 Hz, 3H), 7.73–7.66 (m, 1H), 7.59 (dd, *J* = 10.6, 4.8 Hz, 2H) (Downey et al. 2018). Purity (HPLC): 94.4%.

3-[(1E)-3-Oxo-3-phenylprop-1-en-1-yl]benzotrile (34) Prepared as for **15** from acetophenone (0.50 g, 4.16 mmol) and 3-cyanobenzaldehyde (0.55 g, 4.16 mmol)

to yield the title compound **34** as light yellow crystals (0.63 g, 65%): mp: 113.82 °C (EtOH); ¹H NMR (600 MHz, DMSO) δ 8.51 (s, 1H), 8.20 (dd, *J* = 8.1, 1.0 Hz, 3H), 8.12 (d, *J* = 15.7 Hz, 1H), 7.90 (d, *J* = 7.7 Hz, 1H), 7.77 (d, *J* = 15.7 Hz, 1H), 7.67 (dd, *J* = 12.7, 4.7 Hz, 2H), 7.59 (t, *J* = 7.7 Hz, 2H) (Nagarajan and Shechter 1984). Purity (HPLC): 94.7%.

(2E)-3-[4-(Morpholin-4-yl)phenyl]-1-phenylprop-2-en-1-one (35) Prepared as for **15** from acetophenone (0.50 g, 4.16 mmol) and 4-(4-morpholinyl)benzaldehyde (0.80 g, 4.16 mmol) to yield the title compound **35** as bright yellow crystals (0.15 g, 13%): mp: 149.99 °C (EtOH); ¹H NMR (600 MHz, DMSO) δ 8.14–8.09 (m, 2H), 7.78–7.61 (m, 5H), 7.55 (t, *J* = 7.7 Hz, 2H), 6.99 (d, *J* = 8.9 Hz, 2H), 3.77–3.71 (m, 4H), 3.28–3.22 (m, 4H) (Li et al. 2017). Purity (HPLC): 99.2%.

(2E)-3-(2H-1,3-benzodioxol-5-yl)-1-(3-methoxyphenyl)prop-2-en-1-one (36) Prepared as for **15** from 3-methoxyacetophenone (0.50 g, 3.33 mmol) and 3,4-(methylenedioxy)benzaldehyde (0.50 g, 3.33 mmol) to yield the title compound **36** as bright yellow crystals (0.92 g, 98%): mp: 77.10 °C (EtOH); ¹H NMR (600 MHz, CDCl₃) δ 7.73 (d, *J* = 15.5 Hz, 1H), 7.58 (d, *J* = 7.6 Hz, 1H), 7.53 (s, 1H), 7.43–7.31 (m, 2H), 7.16 (s, 1H), 7.12 (d, *J* = 7.9 Hz, 2H), 6.84 (d, *J* = 7.5 Hz, 1H), 6.02 (s, 2H), 3.88 (s, 3H) (Ruparelia et al. 2018). Purity (HPLC): 99.1%.

Synthesis of 37–41

(2E)-1-(3-Aminophenyl)-3-(2-bromophenyl)prop-2-en-1-one (37) 3'-Aminoacetophenone (0.50 g, 3.70 mmol) and 2-bromobenzaldehyde (0.68 g, 3.70 mmol) were suspended in MeOH (4 mL) and HCl (32 wt.% in H₂O, FCC, 6 mL). The subsequent reaction mixture was mechanically stirred at 120 °C under reflux while being continuously monitored by TLC. Upon completion, the reaction mixture was cooled to room temperature, ice (15 g) was added and the resulting precipitate was filtered, dried (30 °C) and recrystallized from a suitable solvent to yield the title compound **37** as dark brown powder (1.10 g, 99%): mp: 189.86 °C (EtOH); ¹H NMR (600 MHz, DMSO) δ 8.21–8.12 (m, 2H), 8.01 (d, *J* = 15.5 Hz, 1H), 7.95 (s, 1H), 7.91 (d, *J* = 15.5 Hz, 1H), 7.75 (d, *J* = 7.9 Hz, 1H), 7.64 (t, *J* = 7.8 Hz, 1H), 7.58 (dd, *J* = 8.1, 0.8 Hz, 1H), 7.50 (t, *J* = 7.5 Hz, 1H), 7.44–7.37 (m, 1H); ¹³C NMR (151 MHz, DMSO) δ 188.30, 141.78, 138.30, 133.80, 133.34, 132.35, 130.19, 128.76, 128.26, 126.55, 126.49, 125.44, 124.70, 121.31. APCI-HRMS *m/z* calculated for C₁₅H₁₃BrNO [M+H]⁺: 302.0175, found: 302.0176. Purity (HPLC): 99.8%.

(2E)-1-(3-Aminophenyl)-3-(3-bromophenyl)prop-2-en-1-one (38) Prepared as for **37** from 3'-aminoacetophenone (0.50 g, 3.70 mmol) and 3-bromobenzaldehyde (0.68 g, 3.70 mmol) to yield the title compound **38** as light brown powder (0.80 g, 72%): mp: 176.78 °C (EtOH); ¹H NMR (600 MHz, DMSO) δ 8.26–8.13 (m, 2H), 7.97 (d, *J*=15.7 Hz, 1H), 7.95 (s, 1H), 7.87 (d, *J*=7.8 Hz, 1H), 7.73 (d, *J*=15.7 Hz, 1H), 7.64 (t, *J*=7.8 Hz, 2H), 7.58 (d, *J*=7.8 Hz, 1H), 7.43 (t, *J*=7.8 Hz, 1H); ¹³C NMR (151 MHz, DMSO) δ 188.36, 142.82, 138.42, 137.04, 135.23, 133.22, 130.98, 130.91, 130.17, 128.27, 126.72, 126.60, 123.32, 122.40, 121.45. APCI-HRMS *m/z* calculated for C₁₅H₁₃BrNO [M+H]⁺: 302.0175, found: 302.0164. Purity (HPLC): 98.1%.

(2E)-1-(3-Aminophenyl)-3-(2-chlorophenyl)prop-2-en-1-one (39) Prepared as for **37** from 3'-aminoacetophenone (0.50 g, 3.70 mmol) and 2-chlorobenzaldehyde (0.52 g, 3.70 mmol) to yield the title compound **39** as light brown powder (0.94 g, 99%): mp: 188.04 °C (EtOH); ¹H NMR (600 MHz, DMSO) δ 8.23–8.13 (m, 2H), 8.05 (d, *J*=15.6 Hz, 1H), 7.95 (d, *J*=15.6 Hz, 2H), 7.65 (t, *J*=7.8 Hz, 1H), 7.62–7.56 (m, 2H), 7.53–7.43 (m, 2H); ¹³C NMR (151 MHz, DMSO) δ 188.30, 139.05, 138.31, 134.43, 132.20, 132.12, 130.20, 130.08, 128.61, 127.73, 126.63, 126.58, 124.56, 121.39. APCI-HRMS *m/z* calculated for C₁₅H₁₃ClNO [M+H]⁺: 258.0680, found: 258.0673. Purity (HPLC): 99.8%.

(2E)-1-(3-Aminophenyl)-3-(3-chlorophenyl)prop-2-en-1-one (40) Prepared as for **37** from 3'-aminoacetophenone (0.50 g, 3.70 mmol) and 3-chlorobenzaldehyde (0.52 g, 3.70 mmol) to yield the title compound **40** as light brown powder (0.89 g, 93%): mp: 175.73 °C (EtOH); ¹H NMR (600 MHz, DMSO) δ 8.17 (d, *J*=7.6 Hz, 1H), 8.06 (s, 1H), 7.97 (d, *J*=15.7 Hz, 1H), 7.95 (s, 1H), 7.83 (d, *J*=7.3 Hz, 1H), 7.74 (d, *J*=15.7 Hz, 1H), 7.64 (t, *J*=7.8 Hz, 1H), 7.58 (d, *J*=7.9 Hz, 1H), 7.54–7.45 (m, 2H); ¹³C NMR (151 MHz, DMSO) δ 188.39, 142.86, 138.41, 136.78, 133.81, 130.73, 130.32, 130.16, 128.05, 127.90, 126.61, 126.56, 123.36, 121.40. APCI-HRMS *m/z* calculated for C₁₅H₁₃ClNO [M+H]⁺: 258.0680, found: 258.0658. Purity (HPLC): 98.1%.

(2E)-1-(3-Aminophenyl)-3-(3-fluorophenyl)prop-2-en-1-one (41) Prepared as for **37** from 3'-aminoacetophenone (0.50 g, 3.70 mmol) and 3-fluorobenzaldehyde (0.46 g, 3.70 mmol) to yield the title compound **41** as dark brown powder (0.19 g, 21%): mp: 206.07 °C (EtOH); ¹H NMR (600 MHz, DMSO) δ 8.17 (d, *J*=7.7 Hz, 1H), 7.99–7.93 (m, 2H), 7.85 (d, *J*=10.3 Hz, 1H), 7.76 (d, *J*=15.7 Hz, 1H), 7.70 (d, *J*=7.8 Hz, 1H), 7.65 (t, *J*=7.8 Hz, 1H), 7.63–7.57 (m, 1H), 7.55–7.47 (m, *J*=7.9, 6.3 Hz, 1H), 7.30 (td, *J*=8.5,

2.4 Hz, 1H); ¹³C NMR (151 MHz, DMSO) δ 188.43, 163.28, 161.67, 143.14, 138.43, 137.12, 137.07, 135.17, 130.93, 130.88, 130.19, 126.74, 126.66, 125.61, 123.29, 121.54, 117.54, 117.40, 114.83, 114.69. APCI-HRMS *m/z* calculated for C₁₅H₁₃FNO [M+H]⁺: 242.0976, found: 242.0956. Purity (HPLC): 96.4%.

Synthesis of 42–47

1-(3-((E)-[(2-Hydroxy-4-methoxyphenyl)methylidene]amino)phenyl)ethan-1-one (42) A solution of 3'-aminoacetophenone (0.50 g, 3.70 mmol) and 2-hydroxy-4-methoxybenzaldehyde (0.56 g, 3.70 mmol) in EtOH (5 mL) was mechanically stirred at room temperature for approximately 5 min before the dropwise addition of KOH (10% (w/v) aqueous solution, 5 mL). The subsequent reaction mixture was mechanically stirred at room temperature and continuously monitored by TLC. Upon completion, the reaction mixture was quenched with crushed ice (15 g) and acidified to pH 2 with HCl (32 wt. % in H₂O, FCC). The subsequent precipitate was collected by vacuum filtration, dried (30 °C) and recrystallized from EtOH to yield the title compound **42** as dark green crystals (0.08 g, 8%): mp: 94.63 °C (EtOH); ¹H NMR (600 MHz, CDCl₃) δ 13.47 (d, *J*=2.0 Hz, 1H), 8.58 (s, 1H), 7.83 (s, 2H), 7.54–7.41 (m, 2H), 7.30 (d, *J*=8.3 Hz, 1H), 6.51 (d, *J*=8.0 Hz, 2H), 3.85 (s, 3H), 2.64 (s, 3H); ¹³C NMR (151 MHz, CDCl₃) δ 197.84, 164.45, 163.95, 162.75, 149.21, 138.47, 133.96, 129.76, 126.32, 126.21, 120.41, 113.11, 107.54, 101.24, 55.65, 26.85. APCI-HRMS *m/z* calculated for C₁₆H₁₆NO₃ [M+H]⁺: 270.1125, found: 270.1116. Purity (HPLC): 99.8%.

1-(3-((Z)-[(2-Hydroxy-5-methoxyphenyl)methylidene]amino)phenyl)ethan-1-one (43) Prepared as for **42** from 3'-aminoacetophenone (0.50 g, 3.70 mmol) and 2-hydroxy-5-methoxybenzaldehyde (0.56 g, 3.70 mmol) to yield compound **43** as dark red crystals (0.59 g, 59%): mp: 92.81 °C (EtOH); ¹H NMR (600 MHz, CDCl₃) δ 12.53 (s, 1H), 8.63 (s, 1H), 7.86 (d, *J*=11.7 Hz, 2H), 7.52 (t, *J*=7.6 Hz, 1H), 7.47 (d, *J*=7.8 Hz, 1H), 7.02 (d, *J*=9.0 Hz, 1H), 6.97 (d, *J*=8.9 Hz, 1H), 6.91 (s, 1H), 3.81 (s, 3H), 2.65 (s, 3H); ¹³C NMR (151 MHz, CDCl₃) δ 197.73, 163.63, 155.57, 152.50, 149.20, 138.48, 129.86, 126.84, 126.37, 121.20, 120.44, 118.63, 118.32, 115.52, 56.08, 26.91. APCI-HRMS *m/z* calculated for C₁₆H₁₆NO₃ [M+H]⁺: 270.1125, found: 270.1112. Purity (HPLC): 94.4%.

1-(3-((E)-[(3-Bromo-5-chlorophenyl)methylidene]amino)phenyl)ethan-1-one (44) Prepared as for **42** from 3'-aminoacetophenone (0.50 g, 3.70 mmol) and 3-bromo-5-chlorosalicylaldehyde (0.87 g, 3.70 mmol) to yield the title compound **44** as light orange crystals (0.42 g, 32%): mp: 183.31 °C (EtOH); ¹H NMR (600 MHz, CDCl₃) δ 14.07

(s, 1H), 8.61 (s, 1H), 7.95–7.84 (m, 2H), 7.64 (s, 1H), 7.56 (t, $J=7.7$ Hz, 1H), 7.49 (d, $J=7.8$ Hz, 1H), 7.38 (s, 1H), 2.65 (s, 3H); ^{13}C NMR (151 MHz, CDCl_3) δ 197.38, 161.58, 156.92, 147.57, 138.65, 136.12, 130.85, 130.11, 127.76, 126.39, 124.20, 120.40, 120.01, 112.03, 26.90. APCI-HRMS m/z calculated for $\text{C}_{15}\text{H}_{13}\text{ClNO}_2$ $[\text{M}+\text{H}]^+$: 351.9734, found: 351.9714. Purity (HPLC): 99.7%.

1-(3-((E)-[(5-Chloro-2-hydroxyphenyl)methylidene]amino)phenyl)ethan-1-one (45) Prepared as for **42** from 3'-aminoacetophenone (0.50 g, 3.70 mmol) and 5-chlorosalicylaldehyde (0.58 g, 3.70 mmol) to yield the title compound **45** as light orange crystals (0.18 g, 18%): mp: 118.02 °C (EtOH); ^1H NMR (600 MHz, CDCl_3) δ 12.97 (s, 1H), 8.61 (s, 1H), 7.92–7.82 (m, 2H), 7.54 (t, $J=7.7$ Hz, 1H), 7.48 (d, $J=7.8$ Hz, 1H), 7.39 (s, 1H), 7.34 (d, $J=8.8$ Hz, 1H), 6.99 (d, $J=8.8$ Hz, 1H), 2.65 (s, 3H); ^{13}C NMR (151 MHz, CDCl_3) δ 197.56, 162.59, 159.84, 148.66, 138.57, 133.51, 131.60, 129.94, 127.23, 126.22, 124.01, 120.58, 119.86, 119.08, 26.91. APCI-HRMS m/z calculated for $\text{C}_{15}\text{H}_{13}\text{ClNO}_2$ $[\text{M}+\text{H}]^+$: 274.0629, found: 274.0629. Purity (HPLC): 100%.

1-{3-[(E)-[4-(Diethylamino)-2-hydroxyphenyl]methylidene]amino}phenyl}ethan-1-one (46) Prepared as for **42** from 3'-aminoacetophenone (0.50 g, 3.70 mmol) and 4-(diethylamino)salicylaldehyde (0.71 g, 3.70 mmol) to yield the title compound **46** as gold crystals (0.46 g, 42%): mp: 117.85 °C (EtOH); ^1H NMR (600 MHz, CDCl_3) δ 13.52 (s, 1H), 8.47 (s, 1H), 7.84–7.73 (m, 2H), 7.50–7.38 (m, 2H), 7.18 (d, $J=8.7$ Hz, 1H), 6.26 (d, $J=8.8$ Hz, 1H), 6.20 (s, 1H), 3.41 (q, $J=7.0$ Hz, 4H), 2.63 (s, 3H), 1.21 (t, $J=7.0$ Hz, 6H); ^{13}C NMR (151 MHz, CDCl_3) δ 197.89, 163.87, 161.38, 152.00, 149.49, 138.15, 133.95, 129.39, 125.85, 125.17, 120.03, 108.90, 103.90, 97.61, 44.55, 26.72, 12.63. APCI-HRMS m/z calculated for $\text{C}_{19}\text{H}_{23}\text{N}_2\text{O}_2$ $[\text{M}+\text{H}]^+$: 311.1754, found: 311.1746. Purity (HPLC): 100%.

1-(3-((E)-[(2H-1,3-benzodioxol-5-yl)methylidene]amino)phenyl)ethan-1-one (47) Prepared as for **42** from 3'-aminoacetophenone (0.50 g, 3.70 mmol) and 3,4-(methylenedioxy)benzaldehyde (0.56 g, 3.70 mmol) to yield the title compound **47** as light green crystals (0.98 g, 99%): mp: 127.64 °C (EtOH); ^1H NMR (600 MHz, CDCl_3) δ 7.81 (d, $J=15.6$ Hz, 1H), 7.49–7.32 (m, 4H), 7.21 (d, $J=7.9$ Hz, 1H), 6.99 (d, $J=8.0$ Hz, 1H), 6.94 (d, $J=7.7$ Hz, 1H), 6.13 (s, 2H), 3.93 (s, 2H), 3.82 (q, $J=6.9$ Hz, 1H); ^{13}C NMR (151 MHz, CDCl_3) δ 190.69, 149.97, 148.53, 146.93, 144.50, 139.67, 129.59, 129.54, 125.28, 120.54, 119.41, 118.91, 114.52, 108.79, 106.79, 101.75, 58.61, 18.58. APCI-HRMS m/z calculated for $\text{C}_{16}\text{H}_{14}\text{NO}_3$ $[\text{M}+\text{H}]^+$: 268.0968, found: 268.0951. Purity (HPLC): 90.4%.

Biology

In vitro evaluation

Materials

All reagents were commercially available and purchased from various manufacturers. Radioligands [^3H]DPCPX (specific activity 120 Ci/mmol) and [^3H]NECA (specific activity 21.1 Ci/mmol) were obtained from PerkinElmer. Radioactivity was counted by a Packard Tri-CARB 2810 liquid scintillation counter.

Ethics

The collection of tissue samples for the A_1 and $\text{A}_{2\text{A}}$ AR radioligand binding assays were approved by the Health Sciences Ethics Office for Research, Training and Support, North-West University (application number NWU-00260-17-A5) and were performed in accordance with the guidelines of the South African National Standard (SANS) document (The care and use of animals for scientific purposes).

Tissue samples

Male Sprague–Dawley rats were dissected to attain rat whole brain membranes (excluding cerebellum and brain stem) and rat striatal membranes for the A_1 and $\text{A}_{2\text{A}}$ AR radioligand binding assays, respectively. Tissue samples were prepared and stored as described in literature (Van der Walt and Terre'Blanche 2015). Protein concentrations were determined according to the Bradford assay, using bovine serum albumin as reference standard (Bradford 1976).

Adenosine A_1 and $\text{A}_{2\text{A}}$ receptor radioligand binding assays

The degree of binding affinity the test compounds possess towards rat A_1 and $\text{A}_{2\text{A}}$ ARs were determined via radioligand binding assays, as described previously (Bradford 1976; Bruns 1987; Bruns and Watson 2012; Van der Walt and Terre'Blanche 2015). The A_1 AR radioligand binding assay used rat whole brain membranes (expressing A_1 ARs) and 0.1 nM 1,3- $[\text{^3H}]$ -dipropyl-8-cyclopentylxanthine ($[\text{^3H}]$ DPCPX) as radioligand (Bruns 1987) and, in turn, the $\text{A}_{2\text{A}}$ AR radioligand binding assay used rat striatal membranes (expressing $\text{A}_{2\text{A}}$ ARs) and 4 nM 5'- N -ethylcarboxamido $[\text{^3H}]$ adenosine ($[\text{^3H}]$ NECA) as radioligand (Bruns et al. 1986). N^6 -Cyclopentyladenosine (CPA) was also added to the $\text{A}_{2\text{A}}$ AR radioligand binding assay (in order to eliminate the A_1 component of binding exhibited by the non-selective $[\text{^3H}]$ NECA) as well as MgCl_2 (in order to increase radioligand

binding and decrease non-specific binding) (Bruns et al. 1986). The final volume of all incubations contained 1 mL 50 mM Tris.HCl buffer and 1% DMSO (Van der Walt and Terre'Blanche 2015). Non-specific binding of [³H]DPCPX and [³H]NECA for the radioligand binding assays were defined as binding in the presence of 100 μM CPA (Bruns et al. 1986; Van der Walt and Terre'Blanche 2015). Specific binding was defined as the total binding minus the non-specific binding (Van der Walt and Terre'Blanche 2015).

Guanosine triphosphate (GTP) shift assays

The type of binding affinity test compounds exhibited at the rat A₁ AR was determined via a guanosine triphosphate (GTP) shift assay, as described previously (Lohse et al. 1987; Van der Walt and Terre'Blanche 2015; Van der Werden et al. 1995). A GTP shift assay resembles the A₁ AR radioligand binding assay. However, it requires the addition of 100 μM GTP. Non-specific binding was defined as binding in the presence of 10 μM DPCPX (Van der Werden et al. 1995; Lohse et al. 1984).

Statistical data analyses

In short, all statistical data analyses were done using Microsoft Excel and GraphPad Prism Software. Sigmoidal dose response curves, from which IC₅₀ values were calculated, were obtained by plotting the specific binding against the logarithm of the test compounds' concentrations. Subsequently, the IC₅₀ values were used to calculate the K_i values for the competitive inhibition of [³H]DPCPX (K_d = 0.36 nM) against rat whole brain membranes and [³H]NECA (K_d = 15.3 nM) against rat striatal membranes by the test compounds by means of the Cheng–Prusoff equation. All calculated K_i values were determined in triplicate and given as mean ± standard error of the mean (SEM). Specific binding (%) of the radioligand at a maximum tested concentration of 100 μM were determined in duplicate and expressed as the mean in %. SI index values were calculated as a ratio of the A₁ and A_{2A} AR K_i values of test compounds. GTP shifts were calculated by dividing the K_i values of compounds reported in the presence of GTP by the K_i values obtained in the absence of GTP.

In silico evaluation

SwissADME (<https://www.swissadme.ch>), a free web tool, was used to evaluate key parameters of small molecules; such as pharmacokinetics, drug-likeness and medicinal chemistry friendliness. Pharmacokinetic parameters (absorption, distribution, metabolism and excretion), among others, were predicted from molecular structures using the most

relevant computational methods, and thus, do not focus on just one specific property or model (Daina et al. 2017).

Conclusions

A total of 33 chalcones (15–36 and 37–41) and structurally related compounds (42–47) with different substitutions on ring A and/or benzylidene ring B were synthesised, characterized and evaluated in vitro to determine the degree and type of A₁ and A_{2A} receptor binding. While most compounds were not novel, the application of all compounds is original. The chalcone derivatives 24, 29, 37 and 38 possessed selective A₁ affinity below 10 μM; compound 38 was the most potent selective A₁ AR antagonist (K_i (r) = 1.6 μM). Most of the test compounds showed poor A₁ and/or A_{2A} AR affinity upon in vitro evaluation—making it difficult to determine SARs; however, some broad conclusions were drawn from these results. The type of substitution on ring A of the chalcone scaffold played a key role in affinity, and the position of the substitution on benzylidene ring B; the NH₂-group at position C3 of ring A of the chalcone scaffold, and the Br-atom at position C3' on benzylidene ring B were essential to selective A₁ AR affinity (exemplified by compound 27 versus 38 and 37 versus 38). Selective A₁ AR affinity and antagonistic activity may be added to the known biological activities of compounds 24 and 29. The physicochemical and pharmacokinetic properties (based on in silico evaluation) proved the chalcone derivatives 24, 29, 37 and 38, although drug-like, not at all lead-like (29). Thus far, the chalcone chemical structure was a promising scaffold in medicinal chemistry; due to the diverse chemistry and biology of this α,β-unsaturated carbonyl system. The said system may be troublesome (it is perceived as a potential Michael acceptor); however, it easily allows structural modification and introduction of a heterocyclic ring system (such as isoxazole, pyrazole, pyrrole etcetera) which may just be beneficial to A₁ and/or A_{2A} AR binding affinity; thus, leading to the discovery of new pharmacophores from this classes of compounds.

Acknowledgements This study was funded by the National Research Foundation (NRF) of South Africa (Grant number 111814) and the North-West University (NWU). The authors wish to thank Dr D. Otto for NMR analyses and Dr J. Jordaan for MS analyses both from Chemical Research Beneficiation at NWU, as well as Prof. W. Liebenberg for DSC analyses, Prof F. Van der Kooy for HPLC analyses and Ms S. Lowe for assistance with biological assays from the Centre of Excellence for Pharmaceutical Sciences (Pharmacem), NWU.

Compliance with ethical standards

Conflict of interest The authors declare no conflict of interest.

References

- Aarsland D, Pählhagen S, Ballard CG, Ehrt U, Svenningsson P (2012) Depression in Parkinson disease—epidemiology, mechanisms and management. *Nat Rev Neurol* 8:35. <https://doi.org/10.1038/nrneuro.2011.189>
- Aksöz BE, Ertan R (2012) Spectral properties of chalcones II. *Fabrad J Pharm Sci* 37:205–216. <https://www.semanticscholar.org/paper/Spectral-Properties-of-Chalcones-II-Aks%C3%B6z-Ertan/9c63104669fa8cd865bd5c65da7a1d78c8cce36c?p2df>
- Baell JB, Holloway GA (2010) New substructure filters for removal of pan assay interference compounds (PAINS) from screening libraries and for their exclusion in bioassays. *J Med Chem* 53:2719–2740. <https://doi.org/10.1021/jm901137j>
- Barros AI, Silva AM, Alkorta I, Elguero J (2004) Synthesis, experimental and theoretical NMR study of 2'-hydroxychalcones bearing a nitro substituent on their B ring. *Tetrahedron* 60:6513–6521. <https://doi.org/10.1016/j.tet.2004.06.005>
- Batovska DI, Todorova IT (2010) Trends in utilization of the pharmacological potential of chalcones. *Curr Clin Pharmacol* 5:1–29. <https://doi.org/10.2174/157488410790410579>
- Bayer H, Batzl C, Hartman RW, Mannschreck A (1991) New aromatase inhibitors. Synthesis and biological activity of pyridyl-substituted tetralone derivatives. *J Med Chem* 34:2685–2691
- Boison D (2018) Regulation of extracellular adenosine. In: Borea PA, Varani K, Gessi S, Merighi S, Vincenzi F (eds) *The adenosine receptors*, vol 34. The receptors. Humana Press, Totowa, pp 13–58. <https://doi.org/10.1007/978-3-319-90808-3>
- Bradford MM (1976) A rapid and sensitive method for the quantitation of microgram quantities of protein utilizing the principle of protein-dye binding. *Anal Biochem* 72:248–254. [https://doi.org/10.1016/0003-2697\(76\)90527-3](https://doi.org/10.1016/0003-2697(76)90527-3)
- Brenk R, Schipani A, James D, Krasowski A, Gilbert IH, Frearson J, Wyatt PG (2008) Lessons learnt from assembling screening libraries for drug discovery for neglected diseases. *ChemMedChem Chem Enabling Drug Discov* 3:435–444. <https://doi.org/10.1002/cmdc.200700139>
- Bruns RF et al. (1987) Binding of the A₁-selective adenosine antagonist 8-cyclopentyl-1, 3-dipropylxanthine to rat brain membranes. *Naunyn Schmiedeberg's Arch Pharmacol* 335:59–63. https://scholar.google.com/scholar?hl=en&as_sdt=0%2C5&q=Bruns+RF+et+al.+%281987%29+Binding+of+the+A+1-selective+adenosine+antagonist+8-cyclopentyl-1%2C+3-dipropylxanthine+to+rat+brain+membranes+Naunyn-Schmiedeberg%27s+archives+of+pharmacology+335%3A59-63&btnG=
- Bruns RF, Watson IA (2012) Rules for identifying potentially reactive or promiscuous compounds. *J Med Chem* 55:9763–9772. <https://doi.org/10.1021/jm301008n>
- Bruns RF, Lu GH, Pugsley TA (1986) Characterization of the A₂ adenosine receptor labeled by [3H] NECA in rat striatal membranes. *Mol Pharmacol* 29:331–34. https://scholar.google.com/scholar?hl=en&as_sdt=0%2C5&q=Bruns+RF%2C+Lu+GH%2C+Pugsley+TA+%281986%29+Characterization+of+the+A2+adenosine+receptor+labeled+by+%5B3H%5D+NECA+in+rat+striatal+membranes+Molecular+Pharmacology+29%3A331-346&btnG=
- Choi D, Yu S, Baek SH, Kang Y-H, Chang Y-C, Cho H (2016) Synthesis and algicidal activity of new dichlorobenzylamine derivatives against harmful red tides. *Biotechnol Bioprocess Eng* 21:463–476. <https://doi.org/10.1007/s12257-016-0175-8>
- Claisen L, Claparède A (1881) Condensation von Ketonen mit Aldehyden. *Ber Dtsch Chem Ges* 14:2460–2468. <https://doi.org/10.1002/cber.18810140182>
- Clayson DB (1981) Aromatic amines: an assessment of the biological and environmental effects. National Academies Press, Washington D.C. https://scholar.google.com/scholar?hl=en&as_sdt=0%2C5&q=Clayson+DB+%281981%29+Aromatic+amines%3A+an+assessment+of+the+biological+and+environmental+effects.+National+Academies+Press%2C+&btnG=
- Daina A, Zoete V (2016) A boiled-egg to predict gastrointestinal absorption and brain penetration of small molecules. *ChemMedChem* 11:1117–1121. <https://doi.org/10.1002/cmdc.201600182>
- Daina A, Michielin O, Zoete V (2017) SwissADME: a free web tool to evaluate pharmacokinetics, drug-likeness and medicinal chemistry friendliness of small molecules. *Sci Rep* 7:42717. <https://doi.org/10.1038/srep42717>
- de Lera Ruiz M, Lim Y-H, Zheng J (2013) Adenosine A_{2A} receptor as a drug discovery target. *J Med Chem* 57:3623–3650. <https://doi.org/10.1021/jm4011669>
- Dixon AK, Gubitzi AK, Sirinathsinghji DJ, Richardson PJ, Freeman TC (1996) Tissue distribution of adenosine receptor mRNAs in the rat. *Br J Pharmacol* 118:1461–1468. <https://doi.org/10.1111/j.1476-5381.1996.tb15561.x>
- Downey CW, Glist HM, Takashima A, Bottum SR, Dixon GJ (2018) Chalcone and cinnamate synthesis via one-pot enol silane formation-Mukaiyama aldol reactions of ketones and acetate esters. *Tetrahedron Lett* 59:3080–3083. <https://doi.org/10.1016/j.tetlet.2018.06.066>
- Dunwiddie TV (1985) The physiological role of adenosine in the central nervous system. *International review of neurobiology*, vol 27. Elsevier, Amsterdam, pp 63–139. [https://doi.org/10.1016/S0074-7742\(08\)60556-5](https://doi.org/10.1016/S0074-7742(08)60556-5)
- Egan WJ, Merz KM, Baldwin JJ (2000) Prediction of drug absorption using multivariate statistics. *J Med Chem* 43:3867–3877. <https://doi.org/10.1021/jm000292e>
- Fredholm BB et al. (1994) VI. Nomenclature and classification of purinoceptors. *Pharmacol Rev* 46:143. https://scholar.google.com/scholar?hl=en&as_sdt=0%2C5&q=Fredholm+BB+et+al.+%281994%29+VI.+Nomenclature+and+classification+of+purinoceptors+Pharmacological+reviews+46%3A143&btnG=
- Fredholm BB, IJerman AP, Jacobson KA, Klotz K-N, Linden J (2001) International Union of Pharmacology. XXV. Nomenclature and classification of adenosine receptors. *Pharmacol Rev* 53:527–552. https://scholar.google.com/scholar?hl=en&as_sdt=0%2C5&q=Fredholm+BB%2C+IJerman+AP%2C+Jacobson+KA%2C+Klotz+K-N%2C+Linden+J+%282001%29+International+Union+of+Pharmacology.+XXV.+Nomenclature+and+classification+of+adenosine+receptors+Pharmacological+reviews+53%3A527-552&btnG=
- Fredholm BB, IJerman AP, Jacobson KA, Linden J, Müller CE, (2011) International Union of Basic and Clinical Pharmacology. LXXXI. Nomenclature and classification of adenosine receptors—an update. *Pharmacol Rev* 63:1–34. <https://doi.org/10.1124/pr.110.003285>
- Freissmuth M, Schütz W, Linder M (1991) Interactions of the bovine brain A₁-adenosine receptor with recombinant G protein alpha-subunits. Selectivity for rGi alpha-3. *J Biol Chem* 266:17778–17783. https://scholar.google.com/scholar?hl=en&as_sdt=0%2C5&q=Freissmuth+M%2C+Sch%C3%BCtz+W%2C+Linder+M+%281991%29+Interactions+of+the+bovine+brain+A1-adenosine+receptor+with+recombinant+G+protein+alpha-subunits.+Selectivity+for+rGi+alpha-3+Journal+of+Biological+Chemistry+266%3A17778-17783&btnG=
- Furniss B, Hannaford A, Smith P, Tatchell A (1989) Vogel's textbook of practical organic chemistry, 5th edn. Longman Group UK Limited. https://fac.ksu.edu.sa/sites/default/files/vogel_-_practical_organic_chemistry_5th_edition.pdf

- Gaonkar SL, Vignesh U (2017) Synthesis and pharmacological properties of chalcones: a review. *Res Chem Intermed* 43:6043–6077. <https://doi.org/10.1007/s11164-017-2977-5>
- Gatch MB, Wallis CJ, Lal H (1999) The effects of adenosine ligands R-PIA and CPT on ethanol withdrawal. *Alcohol* 19:9–14. [https://doi.org/10.1016/S0741-8329\(99\)00009-9](https://doi.org/10.1016/S0741-8329(99)00009-9)
- Ghose AK, Viswanadhan VN, Wendoloski JJ (1999) A knowledge-based approach in designing combinatorial or medicinal chemistry libraries for drug discovery. I A qualitative and quantitative characterization of known drug databases. *J Comb Chem* 1:55–68. <https://doi.org/10.1021/cc9800071>
- Gomes MN et al (2017) Chalcone derivatives: promising starting points for drug design. *Molecules* 22:1210. <https://doi.org/10.3390/molecules22081210>
- Gütschow M et al (2012) Benzothiazinones: a novel class of adenosine receptor antagonists structurally unrelated to xanthine and adenine derivatives. *J Med Chem* 55:3331–3341. <https://doi.org/10.1021/jm300029s>
- Hallgas B et al (2005) Characterization of lipophilicity and antiproliferative activity of E-2-arylmethylene-1-tetralones and their heteroanalogues. *J Chromatogr B* 819:283–291. <https://doi.org/10.1016/j.jchromb.2005.02.014>
- Hann MM, Keserü GM (2012) Finding the sweet spot: the role of nature and nurture in medicinal chemistry. *Nat Rev Drug Discov* 11:355. <https://doi.org/10.1038/nrd3701>
- Hollenberg PF (2002) Characteristics and common properties of inhibitors, inducers, and activators of CYP enzymes. *Drug Metab Rev* 34:17–35. <https://doi.org/10.1081/DMR-120001387>
- Huang SM et al (2008) New era in drug interaction evaluation: US Food and Drug Administration update on CYP enzymes, transporters, and the guidance process. *J Clin Pharmacol* 48:662–670. <https://doi.org/10.1177/0091270007312153>
- Jackson CE (2011) Cholinergic system. In: Kreutzer JS, DeLuca J, Caplan B (eds) *Encyclopedia of clinical neuropsychology*. Springer, New York, pp 562–564. https://doi.org/10.1007/978-0-387-79948-3_1113
- Jacobson KA, Gao Z-G (2006) Adenosine receptors as therapeutic targets. *Nat Rev Drug Discov* 5:247. <https://doi.org/10.1038/nrd1983>
- Jacobson KA, Moro S, Manthey JA, West PL, Ji X-d (2002) Interactions of flavones and other phytochemicals with adenosine receptors. *Flavonoids in cell function*. Springer, Berlin, pp 163–171. https://doi.org/10.1007/978-1-4757-5235-9_15
- Jain N, Kemp N, Adeyemo O, Buchanan P, Stone TW (1995) Anxiolytic activity of adenosine receptor activation in mice. *Br J Pharmacol* 116:2127–2133. <https://doi.org/10.1111/j.1476-5381.1995.tb16421.x>
- Janse van Rensburg H, Terre'Blanche G, van der Walt M, Legoabe L (2017) 5-Substituted 2-benzylidene-1-tetralone analogues as A1 and/or A2A antagonists for the potential treatment of neurological conditions. *Bioorg Chem* 74:251–259. <https://doi.org/10.1016/j.bioorg.2017.08.013>
- Janse van Rensburg HD, Legoabe LJ, Terre'Blanche G, Van der Walt MM (2019a) 2-benzylidene-1-indanone analogues as dual adenosine A1/A2a receptor antagonists for the potential treatment of neurological conditions. *Drug Res* 69(7):382–391. <https://doi.org/10.1055/a-0808-3993>
- Janse van Rensburg HD, Legoabe LJ, Terre'Blanche G, Van der Walt MM (2019b) Methoxy substituted 2-benzylidene-1-indanone derivatives as A1 and/or A2A AR antagonists for the potential treatment of neurological conditions. *Medchemcomm* 10(2):300–309. <https://doi.org/10.1039/C8MD00540K>
- Johansson B et al (2001) Hyperalgesia, anxiety, and decreased hypoxic neuroprotection in mice lacking the adenosine A1 receptor. *Proc Natl Acad Sci* 98:9407–9412. <https://doi.org/10.1073/pnas.161292398>
- Jung Y, Son K-I, Oh YE, Noh D-Y (2008) Ferrocenyl chalcones containing anthracenyl group: synthesis, X-ray crystal structures and electrochemical properties. *Polyhedron* 27:861–867. <https://doi.org/10.1016/j.poly.2007.11.015>
- Juvale K, Pape VF, Wiese M (2012) Investigation of chalcones and benzochalcones as inhibitors of breast cancer resistance protein. *Bioorg Med Chem* 20:346–355. <https://doi.org/10.1016/j.bmc.2011.10.074>
- Kaplan GB, Cotreau MM, Greenblatt DJ (1992) Effects of benzodiazepine administration on A1 adenosine receptor binding in-vivo and ex-vivo. *J Pharm Pharmacol* 44:700–703. <https://doi.org/10.1111/j.2042-7158.1992.tb05502.x>
- Karaman İ, Gezegen H, Gürdere MB, Dingil A, Ceylan M (2010) Screening of biological activities of a series of chalcone derivatives against human pathogenic microorganisms. *Chem Biodivers* 7:400–408. <https://doi.org/10.1002/cbdv.200900027>
- Karthikeyan C, SH Narayana Moorthy N, Ramasamy S, Vanam U, Manivannan E, Karunagaran D, Trivedi P (2015) Advances in chalcones with anticancer activities. In: *Recent patents on anti-cancer drug discovery*, vol 10. pp 97–115. <https://www.ingentaconnect.com/content/ben/pr/2015/00000010/0000001/art00006>
- Karton Y, Jiang J-I, Ji X-D, Melman N, Olah ME, Stiles GL, Jacobson KA (1996) Synthesis and biological activities of flavonoid derivatives as A3 adenosine receptor antagonists. *J Med Chem* 39:2293–2301. <https://doi.org/10.1021/jm950923i>
- Khanam H (2015) Bioactive Benzofuran derivatives: a review. *Eur J Med Chem* 97:483–504. <https://doi.org/10.1016/j.ejmech.2014.11.039>
- Kirchmair J et al (2015) Predicting drug metabolism: experiment and/or computation? *Nat Rev Drug Discov* 14:387. <https://doi.org/10.1038/nrd4581>
- Klotz K-N, Hessling J, Hegler J, Owman C, Kull B, Fredholm B, Lohse M (1997) Comparative pharmacology of human adenosine receptor subtypes—characterization of stably transfected receptors in CHO cells. Naunyn Schmiedeberg's Arch Pharmacol 357:1–9. https://scholar.google.com/scholar?hl=en&as_sdt=0%2C5&q=Klotz+K-N%2C+Hessling+J%2C+Hegler+J%2C+Owman+C%2C+Kull+B%2C+Fredholm+B%2C+Lohse+M+%281997%29+Comparative+pharmacology+of+human+adenosine+receptor+subtypes%2E%80%93+characterization+of+stably+transfected+receptors+in+CHO+cells+Naunyn-Schmiedeberg%27s+archives+of+pharmacology+357%3A1-9&btnG=
- Langmead CJ et al (2012) Identification of novel adenosine A2A receptor antagonists by virtual screening. *J Med Chem* 55:1904–1909. <https://doi.org/10.1021/jm201455y>
- Legoabe LJ, Van der Walt MM, Terre'Blanche G (2018) Evaluation of 2-benzylidene-1-tetralone derivatives as antagonists of A1 and A2A adenosine receptors. *Chem Biol Drug Design* 91:234–244. <https://doi.org/10.1111/cbdd.13074>
- Li M, Fang D, Geng F, Dai X (2017) Silver-catalyzed efficient synthesis of enamines from propargyl alcohols and amines. *Tetrahedron Lett* 58:4747–4749. <https://doi.org/10.1016/j.tetlet.2017.09.054>
- Lipinski CA, Lombardo F, Dominy BW, Feeney PJ (1997) Experimental and computational approaches to estimate solubility and permeability in drug discovery and development settings. *Adv Drug Deliv Rev* 23:3–25. [https://doi.org/10.1016/S0169-409X\(96\)00423-1](https://doi.org/10.1016/S0169-409X(96)00423-1)
- Liu S, Guo C, Guo Y, Yu H, Greenaway F, Sun M-Z (2014) Comparative binding affinities of flavonoid phytochemicals with bovine serum albumin. *Iran J Pharm Res IJPR* 13:1019. [https://scholar.google.com/scholar?q=Liu+S,+Guo+C,+Guo+Y,+Yu+H,+Greenaway+F,+Sun+M-Z+\(2014\)+Comparative+binding+affinities+of+flavonoid+phytochemicals+with+bovin](https://scholar.google.com/scholar?q=Liu+S,+Guo+C,+Guo+Y,+Yu+H,+Greenaway+F,+Sun+M-Z+(2014)+Comparative+binding+affinities+of+flavonoid+phytochemicals+with+bovin)

- e+serum+albumin+Iranian+journal+of+pharmaceutical+research:+IJPR+13:1019&hl=en&as_sdt=0,5
- Lohse MJ, Lenschow V, Schwabe U (1984) Interaction of barbiturates with adenosine receptors in rat brain. *Naunyn-Schmiedeberg's Arch Pharmacol* 326:69–74. https://scholar.google.com/scholar?hl=en&as_sdt=0%2C5&q=Lohse+MJ%2C+Lenschow+V%2C+Schwabe+U+%281984%29+Interaction+of+barbiturates+with+adenosine+receptors+in+rat+brain+Naunyn-Schmiedeberg%27s+archives+of+pharmacology+326%3A69-74&btnG=
- Lohse MJ, Klotz K-N, Lindenborn-Fotinos J, Reddington M, Schwabe U, Olsson RA (1987) 8-Cyclopentyl-1, 3-dipropylxanthine (DPCPX)—a selective high affinity antagonist radioligand for A1 adenosine receptors. *Naunyn-Schmiedeberg's Arch Pharmacol* 336:204–210. <https://doi.org/10.1007/BF00165806>
- Londos C, Cooper D, Wolff J (1980) Subclasses of external adenosine receptors. *Proc Natl Acad Sci* 77:2551–2554. <https://doi.org/10.1073/pnas.77.5.2551>
- Maemoto T, Finlayson K, Olverman HJ, Akahane A, Horton RW, Butcher SP (1997) Species differences in brain adenosine A1 receptor pharmacology revealed by use of xanthine and pyrazolopyridine based antagonists. *Br J Pharmacol* 122:1202–1208. <https://doi.org/10.1038/sj.bjp.0701465>
- Maemoto T et al (2004) Pharmacological characterization of FR194921, a new potent, selective, and orally active antagonist for central adenosine A1 receptors. *J Pharmacol Sci* 96:42–52. <https://doi.org/10.1254/jphs.FP0040359>
- Martin YC (2005) A bioavailability score. *J Med Chem* 48:3164–3170. <https://doi.org/10.1021/jm0492002>
- Mathew B et al (2019) Perspective design of chalcones for the management of CNS disorders: a mini-review. *CNS Neurol Disord Drug Targets*. <https://doi.org/10.1016/j.cns.2019.11.1246>
- McGrath NA, Brichacek M, Njardarson JT (2010) A graphical journey of innovative organic architectures that have improved our lives. *J Chem Educ* 87:1348–1349. <https://doi.org/10.1021/ed1003806>
- Mellado M et al (2018) Synthesis of chalcones with antiproliferative activity on the SH-SY5Y neuroblastoma cell line: quantitative structure–activity relationship models. *Med Chem Res* 27:2414–2425. <https://doi.org/10.1007/s00044-018-2245-2>
- Montanari F, Ecker GF (2015) Prediction of drug–ABC-transporter interaction—recent advances and future challenges. *Adv Drug Deliv Rev* 86:17–26. <https://doi.org/10.1016/j.addr.2015.03.001>
- Muegge I, Heald SL, Brittelli D (2001) Simple selection criteria for drug-like chemical matter. *J Med Chem* 44:1841–1846. <https://doi.org/10.1021/jm015507e>
- Müller CE (2001) A1 adenosine receptors and their ligands: overview and recent developments. *Il Farmaco* 56:77–80. [https://doi.org/10.1016/S0014-827X\(01\)01005-9](https://doi.org/10.1016/S0014-827X(01)01005-9)
- Munshi R, Pang I-H, Sternweis PC, Linden J (1991) A1 adenosine receptors of bovine brain couple to guanine nucleotide-binding proteins Gi1, Gi2, and Go. *J Biol Chem* 266:22285–22289. https://scholar.google.com/scholar?hl=en&as_sdt=0%2C5&q=Munshi+R%2C+Pang+I-H%2C+Sternweis+PC%2C+Linden+J+%281991%29+A1+adenosine+receptors+of+bovine+brain+couple+to+guanine+nucleotide-binding+proteins+Gi1%2C+Gi2%2C+and+Go+Journal+of+Biological+Chemistry+266%3A22285-22289&btnG=
- Nagarajan M, Shechter H (1984) The diverse carbenic and cationic chemistry of 3-diazo-2, 5-diphenylpyrrole. *J Org Chem* 49:62–74. [https://scholar.google.com/scholar?q=Nagarajan+M,+Shechter+H+\(1984\)+The+diverse+carbenic+and+cationic+chemistry+of+3-diazo-2,+5-diphenylpyrrole+The+Journal+of+Organic+Chemistry+49:62-74&hl=en&as_sdt=0,5](https://scholar.google.com/scholar?q=Nagarajan+M,+Shechter+H+(1984)+The+diverse+carbenic+and+cationic+chemistry+of+3-diazo-2,+5-diphenylpyrrole+The+Journal+of+Organic+Chemistry+49:62-74&hl=en&as_sdt=0,5)
- Nagayama H et al (2019) Effect of istradefylline on mood disorders in Parkinson's disease. *J Neurol Sci* 396:78–83. <https://doi.org/10.1016/j.jns.2018.11.005>
- Nielsen AT, Houlihan WJ (2004) The aldol condensation. *Org React* 16:1–438. <https://doi.org/10.1002/0471264180.or016.01>
- Noji T, Karasawa A, Kusaka H (2004) Adenosine uptake inhibitors. *Eur J Pharmacol* 495:1–16. <https://doi.org/10.1016/j.ejphar.2004.05.003>
- Normile H, Barraco RA (1991) N6-cyclopentyladenosine impairs passive avoidance retention by selective action at A1 receptors. *Brain Res Bull* 27:101–104. [https://doi.org/10.1016/0361-9230\(91\)90288-U](https://doi.org/10.1016/0361-9230(91)90288-U)
- Noyce DS, Pryor WA (1955) Carbonyl reactions. I. Kinetics and mechanism of the acid-catalyzed aldol condensation of benzaldehyde and acetophenone. *J Am Chem Soc* 77:1397–1401. <https://doi.org/10.1021/ja01611a001>
- Opletalova V, Hartl J, Palát K Jr, Patel A (2000) Conformational analysis of 2-hydroxy-2', 5'-diazachalcones. *J Pharm Biomed Anal* 23:55–59. [https://doi.org/10.1016/S0731-7085\(00\)00263-6](https://doi.org/10.1016/S0731-7085(00)00263-6)
- Ottaviani G, Gosling DJ, Patissier C, Rodde S, Zhou L, Faller B (2010) What is modulating solubility in simulated intestinal fluids? *Eur J Pharm Sci* 41:452–457. <https://doi.org/10.1016/j.ejps.2010.07.012>
- Phillis JW (1991) Adenosine and adenine nucleotides as regulators of cellular function. CRC Press Incorporated. https://scholar.google.com/scholar?hl=en&as_sdt=0%2C5&q=Phillis+JW+%281991%29+Adenosine+and+adenine+nucleotides+as+regulators+of+cellular+function.+CRC+press%2C+&btnG=
- Pitsikas N, Borsini F (1997) The adenosine A1 receptor antagonist BIIP 20 counteracts scopolamine-induced behavioral deficits in the passive avoidance task in the rat. *Eur J Pharmacol* 328:19–22. [https://doi.org/10.1016/S0014-2999\(97\)83021-X](https://doi.org/10.1016/S0014-2999(97)83021-X)
- Ralevic V, Burnstock G (1998) Receptors for purines and pyrimidines. *Pharmacol Rev* 50:413–492. https://doi.org/10.1007/978-3-642-28863-0_5
- Rammohan A, Reddy JS, Sravya G, Rao CN, Zyryanov GV (2020) Chalcone synthesis, properties and medicinal applications: a review. *Environ Chem Lett* 18:1–26. <https://doi.org/10.1007/s10311-019-00959-w>
- Ramyashree D, Raghavendra K, Kumar AD, Vagish C, Kumar KA (2017) Synthesis, characterization and antimicrobial activities of chalcones and their post transformation to pyrazole derivatives. *Asian J Chem* 29:1538–1542. https://scholar.google.com/scholar?hl=en&as_sdt=0%2C5&q=Ramyashree+D%2C+Raghavendra+K%2C+Kumar+AD%2C+Vagish+C%2C+Kumar+KA+%282017%29+Synthesis%2C+characterization+n+and+antimicrobial+activities+of+chalcones+and+their+post+transformation+to+pyrazole+derivatives+Asian+J+Chem+29%3A1538-1542&btnG=
- Rao ML, Houjou H, Hiratani K (2001) Novel synthesis of macrocycles with chalcone moieties through mixed aldol reaction. *Tetrahedron Lett* 42:8351–8355. [https://doi.org/10.1016/S0040-4039\(01\)01793-2](https://doi.org/10.1016/S0040-4039(01)01793-2)
- Rao YK, Fang S-H, Tzeng Y-M (2004) Differential effects of synthesized 2'-oxygenated chalcone derivatives: modulation of human cell cycle phase distribution. *Bioorg Med Chem* 12:2679–2686. <https://doi.org/10.1016/j.bmc.2004.03.014>
- Rebola N, Pinheiro PC, Oliveira CR, Malva JO, Cunha RA (2003) Subcellular localization of adenosine A1 receptors in nerve terminals and synapses of the rat hippocampus. *Brain Res* 987:49–58. [https://doi.org/10.1016/S0006-8993\(03\)03247-5](https://doi.org/10.1016/S0006-8993(03)03247-5)
- Reppert SM, Weaver DR, Stehle JH, Rivkees SA (1991) Molecular cloning and characterization of a rat A1-adenosine receptor that is widely expressed in brain and spinal cord. *Mol Endocrinol* 5:1037–1048. <https://doi.org/10.1210/mend-5-8-1037>
- Ritchie TJ, Macdonald SJ, Peace S, Pickett SD, Luscombe CN (2013) Increasing small molecule drug developability in sub-optimal chemical space. *MedChemComm* 4:673–680. <https://doi.org/10.1039/C3MD00003F>

- Robinson SJ, Petzer JP, Terre'Blanche G, Petzer A, Van der Walt MM, Bergh JJ, Lourens AC (2015) 2-Aminopyrimidines as dual adenosine A1/A2A antagonists. *Eur J Med Chem* 104:177–188. <https://doi.org/10.1016/j.ejmech.2015.09.035>
- Ruparella KC et al (2018) The synthesis of chalcones as anticancer prodrugs and their bioactivation in CYP1 expressing breast cancer cells. *Med Chem* 14:322–332. <https://doi.org/10.2174/1573406414666180112120134>
- Sahu NK, Balbhadra S, Choudhary J, Kohli DV (2012) Exploring pharmacological significance of chalcone scaffold: a review. *Curr Med Chem* 19:209–225. <https://doi.org/10.2174/092986712803414132>
- Sankaranarayanan S, Ryan TA (2007) Neuronal exocytosis. Protein trafficking in neurons. Elsevier, Amsterdam, pp 97–124. <https://doi.org/10.1016/B978-012369437-9/50010-4>
- Sawle P, Moulton BE, Jarzykowska M, Green CJ, Foresti R, Fairlamb IJ, Motterlini R (2008) Structure–activity relationships of methoxychalcones as inducers of heme oxygenase-1. *Chem Res Toxicol* 21:1484–1494. <https://doi.org/10.1021/tx800115g>
- Schmidt JG (1881) Ueber die Einwirkung von Aceton auf Furfurol und auf Bittermandelöl bei Gegenwart von Alkalilauge. *Ber Dtsch Chem Ges* 14:1459–1461. <https://doi.org/10.1002/cber.188101401306>
- Shenvi S, Kumar K, Hatti KS, Rijesh K, Diwakar L, Reddy GC (2013) Synthesis, anticancer and antioxidant activities of 2, 4, 5-trimethoxy chalcones and analogues from asaronaldehyde: structure–activity relationship. *Eur J Med Chem* 62:435–442. <https://doi.org/10.1016/j.ejmech.2013.01.018>
- Shimada J et al (1997) Adenosine A2A antagonists with potent anticonvulsant activity. *Bioorg Med Chem Lett* 7:2349–2352. [https://doi.org/10.1016/S0960-894X\(97\)00440-X](https://doi.org/10.1016/S0960-894X(97)00440-X)
- Singh P, Anand A, Kumar V (2014) Recent developments in biological activities of chalcones: a mini review. *Eur J Med Chem* 85:758–777. <https://doi.org/10.1016/j.ejmech.2014.08.033>
- Stroba A et al (2009) 3, 5-Diphenylpent-2-enoic acids as allosteric activators of the protein kinase PDK1: structure–activity relationships and thermodynamic characterization of binding as paradigms for PIF-binding pocket-targeting compounds. *J Med Chem* 52:4683–4693. <https://doi.org/10.1021/jm9001499>
- Suwito H et al (2014) Design and synthesis of chalcone derivatives as inhibitors of the ferredoxin–ferredoxin-NADP+ reductase interaction of *Plasmodium falciparum*: pursuing new antimalarial agents. *Molecules* 19:21473–21488. <https://doi.org/10.3390/molecules191221473>
- Suzuki F et al. (1993) Adenosine A1 antagonists. 3. Structure-activity relationships on amelioration against scopolamine- or N6-[(R)-phenylisopropyl] adenosine-induced cognitive disturbance. *J Med Chem* 36:2508–2518. https://scholar.google.com/scholar?hl=en&as_sdt=0%2C5&q=Suzuki+F+et+al.+%281993%29+Adenosine+A1+antagonists+.+3.+Structure-activity+relationships+on+amelioration+against+scopolamine-or+N6-%5B%28R%29-phenylisopropyl%5D+adenosine-induced+cognitive+disturbance+Journal+of+medicinal+chemistry+36%3A2508-2518&btnG=
- Swanson TH, Drazba JA, Rivkees SA (1995) Adenosine A1 receptors are located predominantly on axons in the rat hippocampal formation. *J Comp Neurol* 363:517–531. <https://doi.org/10.1002/cne.903630402>
- Szakács G, Váradi A, Özvegy-Laczka C, Sarkadi B (2008) The role of ABC transporters in drug absorption, distribution, metabolism, excretion and toxicity (ADME–Tox). *Drug Discov Today* 13:379–393. <https://doi.org/10.1016/j.drudis.2007.12.010>
- Szopa A et al (2018) DPCPX, a selective adenosine A1 receptor antagonist, enhances the antidepressant-like effects of imipramine, escitalopram, and reboxetine in mice behavioral tests. *Naunyn Schmiedeberg's Arch Pharmacol* 391:1361–1371. <https://doi.org/10.1007/s00210-018-1551-z>
- Szopa A et al (2019) Agomelatine and tianeptine antidepressant activity in mice behavioral despair tests is enhanced by DMPX, a selective adenosine A2A receptor antagonist, but not DPCPX, a selective adenosine A1 receptor antagonist. *Pharmacol Rep* 71:676–681. <https://doi.org/10.1016/j.pharep.2019.03.007>
- Teague SJ, Davis AM, Leeson PD, Oprea T (1999) The design of leadlike combinatorial libraries. *Angew Chem Int Ed* 38:3743–3748. [https://doi.org/10.1002/\(SICI\)1521-3773\(19991216\)38:24%3c3743::AID-ANIE3743%3e3.0.CO;2-U](https://doi.org/10.1002/(SICI)1521-3773(19991216)38:24%3c3743::AID-ANIE3743%3e3.0.CO;2-U)
- Testa B, Kraemer S (2007) The biochemistry of drug metabolism—an introduction—testa-2007-chemistry and biodiversity-Wiley Online Library. *Chem Biodivers*. <https://doi.org/10.1002/cbdv.200890199>
- Unoh Y, Hirano K, Satoh T, Miura M (2013) Palladium-catalyzed decarboxylative arylation of benzoylacrylic acids toward the synthesis of chalcones. *J Org Chem* 78:5096–5102. <https://doi.org/10.1021/jo400716e>
- Van Calker D, Müller M, Hamprecht B (1978) Adenosine inhibits the accumulation of cyclic AMP in cultured brain cells. *Nature* 276:839. https://scholar.google.com/scholar?hl=en&as_sdt=0%2C5&q=Van+Calker+D+%2C+M%C3%BCller+r+M%2C+Hamprecht+B+%281978%29+Adenosine+inhibits+the+accumulation+of+cyclic+AMP+in+cultured+brain+cells+Nature+276%3A839&btnG=
- Van der Walt MM, Terre'Blanche G (2015) 1, 3, 7-Triethyl-substituted xanthines—possess nanomolar affinity for the adenosine A1 receptor. *Bioorg Med Chem* 23:6641–6649. <https://doi.org/10.1016/j.bmc.2015.09.012>
- Van der Werden EM et al (1995) 8-Substituted adenosine and theophylline-7-riboside analogues as potential partial agonists for the adenosine A1 receptor. *Eur J Pharmacol Mol Pharmacol* 290:189–199. [https://doi.org/10.1016/0922-4106\(95\)00064-X](https://doi.org/10.1016/0922-4106(95)00064-X)
- Vásquez-Martínez YA et al (2019) Antimicrobial, anti-inflammatory and antioxidant activities of polyoxygenated chalcones. *J Braz Chem Soc* 30:286–304. <https://doi.org/10.21577/0103-5053.20180177>
- Vazquez-Rodriguez S, Matos MJ, Santana L, Uriarte E, Borges F, Kachler S, Klotz KN (2013) Chalcone-based derivatives as new scaffolds for h A3 adenosine receptor antagonists. *J Pharm Pharmacol* 65:697–703. <https://doi.org/10.1111/jphp.12028>
- Veber DF, Johnson SR, Cheng H-Y, Smith BR, Ward KW, Kopple KD (2002) Molecular properties that influence the oral bioavailability of drug candidates. *J Med Chem* 45:2615–2623. <https://doi.org/10.1021/jm020017n>
- Vollert C, Forkuo GS, Bond RA, Eriksen JL (2013) Chronic treatment with DPCPX, an adenosine A1 antagonist, worsens long-term memory. *Neurosci Lett* 548:296–300. <https://doi.org/10.1016/j.neulet.2013.05.052>
- Von Lubitz DK, Paul IA, Bartus RT, Jacobson KA (1993) Effects of chronic administration of adenosine A1 receptor agonist and antagonist on spatial learning and memory. *Eur J Pharmacol* 249:271. [https://doi.org/10.1016/0014-2999\(93\)90522-J](https://doi.org/10.1016/0014-2999(93)90522-J)
- Wang T, Chen G, Lu YJ, Chen Q, Huo Y, Li X (2019) Intermolecular multiple dehydrogenative cross-couplings of ketones with boronic acids and amines via copper catalysis. *Adv Synth Catal* 361:3886–3892. <https://doi.org/10.1002/adsc.201900419>
- Wu S, Yu H, Hu Q, Yang Q, Xu S, Liu T (2017) Silver-catalyzed decarboxylative cross-coupling of α -keto acids with alkenes giving approach to chalcones. *Tetrahedron Lett* 58:4763–4765. <https://doi.org/10.1016/j.tetlet.2017.11.005>
- Xie Z et al (2017) Synthesis and evaluation of hydroxychalcones as multifunctional non-purine xanthine oxidase inhibitors for the treatment of hyperuricemia. *Bioorg Med Chem Lett* 27:3602–3606. <https://doi.org/10.1016/j.bmcl.2017.01.053>

- Yacoubi ME, Ledent C, Parmentier M, Bertorelli R, Ongini E, Costentin J, Vaugeois JM (2001) Adenosine A2A receptor antagonists are potential antidepressants: evidence based on pharmacology and A2A receptor knockout mice. *Br J Pharmacol* 134:68–77. <https://doi.org/10.1038/sj.bjp.0704240>
- Zhang N, Yang D, Wei W, Yuan L, Nie F, Tian L, Wang H (2015) Silver-catalyzed double-decarboxylative cross-coupling of α -keto acids with cinnamic acids in water: a strategy for the preparation of chalcones. *J Org Chem* 80:3258–3263. <https://doi.org/10.1021/jo502642n>
- Zhou B, Xing C (2015) Diverse molecular targets for chalcones with varied bioactivities. *Med Chem* 5:388. <https://doi.org/10.4172/2161-0444.1000291>
- Zhou Y, Li Z, Yang X, Chen X, Li M, Chen T, Yin S-F (2016) Phosphorous acid promoted hydration–condensation of aromatic alkynes with aldehydes affording chalcones in an oil/water two-phase system. *Synthesis* 48:231–237. <https://doi.org/10.1055/s-0035-1560832>
- Zhuang C, Zhang W, Sheng C, Zhang W, Xing C, Miao Z (2017) Chalcone: a privileged structure in medicinal chemistry. *Chem Rev* 117:7762–7810. <https://doi.org/10.1021/acs.chemrev.7b00020>

Publisher's Note Springer Nature remains neutral with regard to jurisdictional claims in published maps and institutional affiliations.